Julius-Maximilians-Universität Würzburg

Institut für Geographie und Geologie

Physische Geographie

Prof. Dr. Heiko Paeth

Dynamic Statistical Modelling of Climate-Related Glacier Mass Balance Changes in Norway

Dissertation zur Erlangung des

naturwissenschaftlichen Doktorgrades

der Bayerischen Julius-Maximilians-Universität Würzburg

vorgelegt von

Sebastian Mutz

aus Selb

Würzburg 2013

Eingereicht am:

1. Gutachter:	Prof. Dr. Heiko Paeth
2. Gutachter:	PD Dr. Stefan Winkler

1. Prüfer:	Prof. Dr. Heiko Paeth
2. Prüfer:	Prof. Dr. Hartwig Frimmel

der mündlichen Prüfung

Tag der mündlichen Prüfung: 26/11/2013

Doktorurkunde ausgehändigt am:

Abstract

The glaciers in Norway exert a strong influence on Norwegian economy and society. Unlike many glaciers elsewhere and despite ongoing climate change and warming, many of them showed renewed advances and positive net mass changes in the 1980's and 1990's, followed by rapid retreats and mass losses since 2000. This difference in behaviour may be attributed to differences and shifts in the glaciological regime - the differences in the magnitude of impacts of climatic and non-climatic geographical factors on the glacier mass.

This study investigates the influence of various atmospheric variables on mass balance changes of a selection of glaciers in Norway by means of Pearson correlation analyses and cross-validated stepwise multiple regression analyses. The analyses are carried out for three time periods (1949-2008, 1949-1988, 1989-2008) separately in order to take into consideration the possible shift in the glaciological regime in the 1980's. The atmospheric variables are constructed from ERA40 and NCEP/NCAR re-analysis datasets and include regional means of seasonal air temperature and precipitation rates and atmospheric circulation indices. The multiple regression models trained in these time periods are then applied to predictors reconstructed from the CMIP3 climate model dataset to generate an estimate for mass changes from the year 1950 to 2100. The temporal overlap of estimates and observations is used for calibration. Finally, observed atmospheric states in seasons that are characterised by a particularly positive or negative mass balance are categorised into time periods of modelled climate by the application of a Bayesian classification procedure.

The strongest influence on winter mass balance is exerted by different indices of the North Atlantic Oscillation (NAO), Northern Annular Mode (NAM) and precipitation. The correlation coefficients and explained variances determined from the multiple regression analyses reveal an East-West gradient, suggesting a weaker influence of the NAO and NAM on glaciers underlying a more continental regime. The highest correlation

coefficients and explained variances were obtained for the 1989-2008 time period, which might be due to a strong and predominantly positive phase of the NAO. Multi-model ensemble means of the estimates show a mass loss for all three eastern glaciers, while the estimates for the more maritime glaciers are ambivalent. In general, the estimates show a greater sensitivity to the training time period than to the greenhouse gas emission scenarios according to which the climates were simulated. The average net mass change by the end of 2100 is negative for all glaciers except for the northern Engabreen. For many glaciers, the Bayesian classification of observed atmospheric states into time periods of modelled climate reveals a decrease in probability of atmospheric states favouring extremes in winter, and an increase in probability of atmospheric states favouring extreme mass loss in summer for the distant future (2071-2100). This pattern of probabilities for the ablation season is most pronounced for glaciers underlying a continental and intermediate regime.

Kurzzusammenfassung

Gletscher in Norwegen stellen einen starken Einflussfaktor auf Wirtschaft und Gesellschaft dar. Trotz des Klimawandels und Erwärmung kam es zu einem Vorstoß der Gletscher in den späten 1980er und 1990ern, welcher erst ab dem Jahr 2000 durch einen starken Massenverlust abgelöst wurde. Dieses Verhalten lässt sich möglicherweise durch Unterschiede und Veränderungen im glaziologischen Regime erklären, d.h. Unterschiede in der Stärke der Einflüsse von klimatisch und nicht-klimatischen Faktoren auf die Gletschermassenbilanzen.

Diese Arbeit untersucht den Einfluss verschiedener atmosphärischer Variablen auf die Massenveränderungen einiger Gletscher in Norwegen mit Hilfe von Korrelationsanalysen und kreuzvalidierten schrittweise multiple Regressionsanalysen. Diese werden für die Zeitabschnitte 1949-2008, 1949-1988 und 1989-2008 separat durchgeführt um den möglichen Regimewechsel in the 1980ern zu berücksichtigen. Die atmosphärischen Variablen werden aus ERA40 und NCEP/NCAR Re-analysen erstellt und beinhalten unter anderem atmosphärische Zirkulationsindizes und regionale Mittel von saisonalem Niederschlag und Temperatur. Die Regressionmodelle werden dann auf die aus den Daten des CMIP3 Klimamodelldatenarchiv rekonstruierten Prädiktoren angewandt um eine Abschätzung der Gletschermassenveränderung für den Zeitraum von 1950 bis 2100 zu erstellen. Die zeitliche Überschneidung von Abschätzungen und Beobachtungen wird zur Eichung genutzt. Zuletzt wird durch einen Bayesischen Klassifizierungsansatz beobachtete atmosphärische Zustände in Jahren, die durch besonders negative oder positive Massenbilanzen geprägt sind, in Zeitabschnitte von modelliertem Klima eingeordnet.

Der größte Einfluss auf Wintermassenbilanzen stellt die Nordatlantische Oszillation, Arktische Oszillation und Niederschlagsmittel dar. Die Höhe der Korrelationskoeffizienten und der durch diese Prädiktoren erklärte Varianz der Wintermassenbilanz nimmt für die östlich gelegenen, kontinental geprägteren Gletscher ab. Die stärksten stochastischen Zusammenhänge und höchsten erklärten Varianzen werden aus dem 1989-

2008 Zeitabschnitt gewonnen und lassen sich möglicherweise durch eine meist starke und positive Phase der Winter-NAO in diesem Zeitraum erklären. Multi-model Ensemble Means der Abschätzungen der Gletschermassenveränderungen zeigen den größten Massenverlust für die östlich gelegenen, kontinentaleren Gletscher auf. Die Abschätzungen für die eher maritim geprägten Gletscher sind weniger eindeutig. Im Allgemeinen reagieren die Abschätzungen empfindlicher auf die Wahl des Trainingszeitraums für die Regressionsmodelle als auf die Emissionsszenarien der Klimamodellläufe. Im Durchschnitt ist die kumulative Massenbilanz im Jahr 2100 jedoch für fast alle Gletscher negativ. Der nördlich gelegene Engabreen stellt die einzige Ausnahme dar. Die Resultate des Bayesischen Klassifikationsansatzes zeigen eine Abnahme in der Wahrscheinlichkeit für atmospphärischen Zustände, die Minima und Maxima winterlicher Akkumulation begünstigen. Des Weiteren zeigen die Resultate eine Zunahme in der Wahrscheinlichkeit der atmosphärischen Zustände, die starken Massenverlust im Sommer begünstigen. Dies ist besonders bei den Gletschern der Fall, die einem kontinentalen oder Übergangsregime unterliegen.

Contents

List of Figures

List of Abbreviations

Glaciers

Ålf	Ålfotbreen
Aus	Austdalsbreen
Eng	Engabreen
Grå	Gråsubreen
Han	Hansebreen
Har	Hardangerjøkelen
Hel	Hellstugubreen
Lan	Langfjordjøkelen
Nig	Nigardsbreen
Sto	Storbreen

Acronyms

AO	Arctic Oscillation
AR4	Fourth Assessment Report
BLAS	Basic Linear Algebra Subprograms
CMIP3	Cpuples Model Intercomparison Project, 3rd phase
EA	East Atlantic (pattern)
EA/WR	East Atlantic/Western Russia (pattern)
ECMWF	European Centre for Medium-Range Weather Forecast
EOF	Empirical Orthogonal Functions
ERA-40	ECMWF Re-Analysis, 40 years
IMSL	International Mathematics and Statistical Library
IPCC	International Panel on Climate Change
NAM	Northern Annular Mode
NAO	North Atlantic Oscillation
NAOi	North Atlantic Oscillation index
NCEP	National Centers for Environmental Prediction
NCAR	National Center for Atmospheric Research
NVE	Norges Vassdrags- og Energidirektorat

	(Norwegian Water Resources and Energy Directorate)
PC	Principal Component
PCA	Principal Component Analysis
PCMDI	Program for Climate Model Diagnosis and Intercomparison
PDF	Probability Density Function
PNA	Pacific North American (pattern)
RMSE	Root Mean Square Error
WCRP	World Climate Research Programme

1 Introduction and Background

The first chapter introduces to Norwegian glaciers and their socio-economic importance. Furthermore, it describes the research history of these glaciers and the motivation and aims for this study. The first section provides an overview of the glaciers, their socio-economic relevance, and the motivation for this study. It also outlines the scientific research carried out in the past, including investigations of past- and present-day conditions of the glaciers, as well as predictions made for the future developments of the glacier length- and mass balance changes. The second section describes the aims of this study and how it complements previous studies.

1.1 Glaciers of Norway

Glacier inventories made for northern (ØSTREM et al., 1973) and southern Norway (ØSTREM and ZIEGLER, 1969; ØSTREM et al., 1988) reveal that approximately 2,600 km^2 of the land in Norway is covered by glaciers. About 60% of that glacier area is in South Norway (NVE, 2012). The largest ice cap in Norway is Jostedalsbreen and covers 487km^2 (ØSTREM and HAAKENSEN, 1993). Thee glaciers in Norway are estimated to make up a total volume of approximately 164 km^3 (ØSTREM et al., 1988). They exert a strong influence on society and economy in Norway. In addition to the general risks posed by glacier melting (e.g. LÖFFLER, 1988), the socio-economic relevance of the glaciers is also highlighted by their role in tourism and electricity generation in Norway. Electricity generation from melt water flow contributes ~15% to the hydroelectric power generation in Norway, which currently (2011) makes up more than than 95% of the total power production in the country (SSB, 2012).

The changing climate invokes complex responses in the cryosphere (e.g. BAMBER and PAYNE, 2004). Landsat TM (thematic mapper) scenes reveal an area loss of 23% since 1930 for 38 glaciers that were investigated by ANDREASSEN et al. (2008) and a 9% loss in area of 300 glaciers in the Jostedalsbreen region from 1966 to 2006 (PAUL et al., 2011). The mass the more maritime glaciers of total 42 glaciers investigated by ANREASSEN et al. (2008) show a mass surplus between 1962 and 2000. Since 2001 all monitored glaciers have show a mass deficit and all of last recent advances stopped (ANREASSEN et al., 2008). In the mid-1980's, a change point in cumulative net mass balance has been identified (e.g. FEALY and SWEENEY, 2005) that is characterised by the onset of a net mass surplus of many glaciers. This surplus is particularly high for maritime glaciers (Fig.1.1). While the factors controlling advances during the 1990's are reasonably well understood, the reasons for the most recent retreats are still uncertain (WINKLER et al., 2009). Generally, the observed retreat of many glaciers is viewed as direct consequence of global warming (DYURGEROV and MEIER, 2000; DYURGEROV, 2005; OERLEMANS, 2005). The importance of further investigation into the ongoing changes in length and mass balance of glaciers in response to an evolving climate is stressed by many, including the IPCC (2007), DYURGEROV (2003, 2005) and WINKLER et al. (2010). Ecological impacts and natural hazards resulting from changes in glacial mass (LÖFFLER, 1988) stress the need of reliable estimates for future mass changes in order to establish a basis for policy making. Furthermore, the role of fossil fuels in anthropogenic climate change (e.g. HOUGHTON, et al. 2001) makes the research into renewable energy sources, such as hydropower, an essential part of climate change mitigation efforts (HOFFERT et al., 1998; CALDEIRA et al., 2003; HOFFERT et al., 2003).

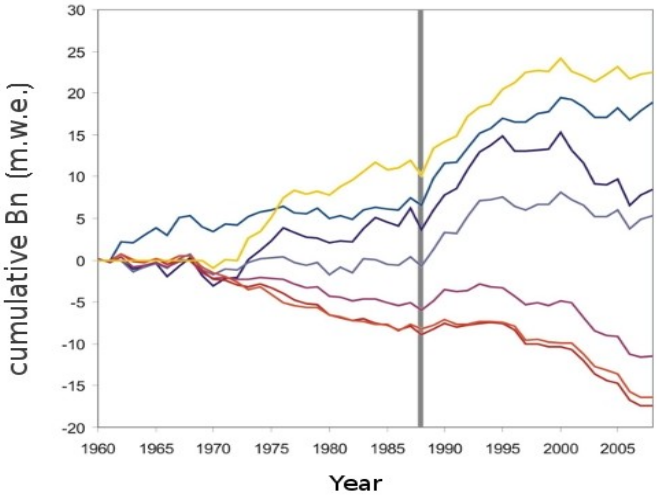

Figure 1.1: Change point in cumulative net mass balance (Bn) of glaciers Engabreen (■), Ålfotbreen (■), Nigardsbreen (■), Hardangerjøkelen (■), Storbreen (■), Hellstugubreen (■), and Gråsubreen (■).

The relationship between glacial dynamics and climate phenomena are subject of much discussion in both glaciological and climatological communities as research status reports such as GUISAN et al. (1995), NESJE and DAHL (2000), OERLEMANS (2001), BAMBER and PAYNE (2004), HUBER et al. (2005) and BARRY (2006) show. In particular, sensitivity analyses and estimates of glacial retreat over the future decades or century are discussed (e.g. HAEBERLI and BENISTON, 1998; HAEBERLI et al., 1998, 1999; HOELZLE et al., 2000; OERLEMANS, 2000, 2001; HOUGHTON et al., 2001; MAISCH, 2002; HAEBERLI and ZUMBÜHL, 2003; MAISCH and HAEBERLI, 2003; WEBER and BRAUN, 2004; SCHULER et al., 2005; ZEMP et al., 2006; NESJE et al. 2008). However, despite intensive study, the different responses of glaciers to climate change still lack understanding and need to be investigated and modelled with consideration of the specific geographical context of each glacier (e.g. WINKLER et al., 2010). There are various approaches to modelling mass balance (KUHN et al., 1999; BAMBER and PAYNE, 2004; MARSHALL, 2006; HAEBERLI et al., 2007) in order to understand present-day climate-glacier dynamics, reconstruct historical mass changes and produce reliable estimates for future mass development. These include methods to calculate the long-term mean net mass balance from few, specific glaciological parameters (e.g. HOELZLE et al., 2007), as well as physical as degree-day models, which use the direct correlation between melting and air temperatures at different vertical levels (WINKLER,

2009). The general disadvantages of energy-balance models, which are primarily developed for glaciers in the European Alps (OERLEMANS, 2001), lie in the requirement of high-resolution meteorological measurements. Another option is the statistical modelling of mass balance using the established statistical relationships between mass balance and various meteorological factors, such as temperature and precipitation, and atmospheric circulation, in particular the North Atlantic Oscillation. These relationships have already been empirically investigated (NESJE, 1989, 1995, 2005; NESJE et al., 1995, 2000; WINKLER, 1996, 1997; POHJOLA and ROGERS, 1997a,b; WINKLER et al., 1997; WASHINGTON et al., 2000, REICHERT et al., 2001; SIX et al., 2001; NESJE and DAHL, 2003; CHINN et al., 2005; FEALY and SWEENEY, 2005) and used to model glacier mass changes (NESJE et al., 1995; NESJE and DAHL, 2003; NORDLI et al., 2003; NESJE, 2005). However, these focus primarily on the reconstruction of glacier mass balance and not on the prediction of mass changes in the future. Only a few studies present future estimates of mass balance changes based on meteorological data (BRAITHWAITE and ZHANG, 1999; SCHNEEBERGER et al., 2001; RADIC and HOCK, 2006; NESJE et al 2008), but these models are either not coupled to climate model simulations or not transferable to the glaciers in this study due to differences in the geographical setting and sensitivity to meteorological factors. Many of the studies carried out in the past involve high mountain glaciers that underlie an intermediate or continental climate. Therefore, conclusions drawn from these may not apply to the many of the glaciers in Norway (WINKLER et al., 1997, WINKLER and HAAKENSEN, 1999; CHINN et al., 2005). For example, the glacial retreat in some regions, which is claimed to have exceeded that of the Holocene (REICHERT et al., 2002) and has been used to support the idea of anthropogenic climate change, could not be observed for maritime high mountain glaciers. Many showed continuous advance (WINKLER et al., 1997), followed by a rapid retreat of glacier fronts only since 2000 (e.g. CHINN et al., 2005; ANDREASSEN et al., 2005; ANDREASSEN et al. 2011). Those differences are largely attributed to differences in the magnitude of impacts of climatic and non-climatic factors on the glaciers' mass balance. This so-called 'glaciological regime' is an expression of a regional

differentiation based on climatic conditions, such as the degree of continentality, but may also be understood as regional differences in weighting of the influences of climatic factors on the glaciers' mass balance (WINKLER, 2009). The maritime glaciers and continental mountain glaciers of southern Norway present a good example of such a differentiation. The air temperature driven ablation of the maritime glaciers on a lower altitude is greater and - in order for the glacier to exist at all - the mass accumulation in winter needs to be higher (Fig.1.2 a,b) than that of the high-altitude glaciers of a more continental regime (WINKLER, 2009). This causes a greater total annual mass exchange (Fig.1.2 c) of those maritime glaciers (ANDREASSEN et al., 2005; WINKLER, 2009).

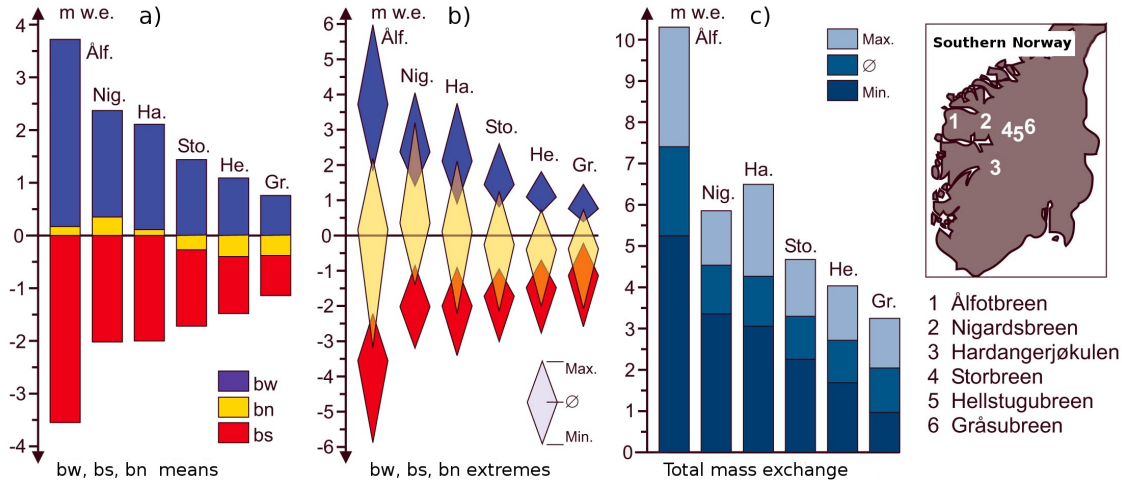

Figure 1.2: a) Mean winter (bw), summer (bs) and net glacier mass balance (bn); b) bw,bs and bn extremes, c) total mass exchange and the geographical location of the glaciers, modified following Winkler (2009).

The different glaciological regimes may explain why energy-balance models that were calibrated for the European Alps (OERLEMANS, 1988; GRUELL, 1989; GRUELL and OERLEMANS, 1989) produce results for the simulation and reconstruction of glacial dynamics of high mountain glaciers in Scandinavia and the Southern Alps (New Zealand) (OERLEMANS, 1986, 1994, 1997) that are in poor agreement with actual observations (NESJE et al., 1995, WINKLER et al., 1997, CHINN et al., 2005). Degree-day models that were developed for maritime glaciers (LAUMANN, 1992; LAUMANN and REEH, 1993; JÓHANNESSON et al., 1995,

JÓHANNESSON, 1997) produce plausible results for maritime Scandinavian glaciers. These models exist for Scandinavian and Alpine glaciers (MAISCH, 2002), but they are not coupled to the available climate modelling results. The more recent reconstructions of mass balance of the Scandinavian glacier Storbreen from a mass balance model by ANDREASSEN and OERLEMANS (2009) are in good agreement with observations. However, the model requires an identification of the most suitable automated weather station prior to reconstruction and does not allow a direct coupling to climate model output. NESJE et al. (2008) provide an estimate for future mass balance changes based on a climate scenario for the period 2071-2100, observations from the 1961-1990 time period and a knowledge of past glacier states from NESJE et al. (2001), DAHL and NESJE (1994, 1996) and BAKKE et al. (2005), and proxy temperature and precipitation reconstructions from BJUNE et al. (2005). However, this method does not take into account the possible change in the glaciological regime of Norwegian glaciers in the late 20th century or different future emission scenarios for climate. The modelling of future climate is based on scenarios that describe the results of different technological and demographic development and physically models the climate accordingly (NAKICENOVIC et al., 2000). The results therefore present the best climatological framework to base estimates of changes in glaciated regions on (HOUGHTON et al., 2001).

1.2 Aims of this Study

This section outlines the aims of this study. Details about the applied methods and further justification for them is provided in chapter 3. The overall aim of this study is to complement previous investigations into climate-glacier dynamics and predictions for the future evolution of glaciers by providing an empirical assessment of the influence of various atmospheric factors on glacier mass balance changes and by generating estimates for future mass balance changes for different scenarios and under consideration of the different glaciological regimes and regional disparities. Future climate model simulations and present-day stochastic

dependences between atmospheric variables and mass balance form the basis of these estimates. Furthermore, present-day atmospheric states favouring summer and winter mass balance minima and maxima are categorised into different time periods of modelled climate, covering present-day and future, in order to assess what type of mass balance changes are most likely to be favoured by modelled atmospheric conditions in different time periods. The data basis for this undertaking is described in chapter 2 and the detailed methods are outlined in chapter 3.

The first aim of this study is to assess the influence of various meteorological and climatic factors on glacier mass balance. This is achieved by relating an independent target variable (predictand), in this case the glacier mass balance, to various causal factors (predictors), in this case various atmospheric variables, by means of a cross-validated stepwise multiple regression analysis. In order to avoid the inclusion of irrelevant factors in the multiple regression analysis, simple correlation analyses help create a pre-selection of predictors. Given the control of large scale circulation associated with precipitation on glacier mass balance in Norway (e.g. NESJE et al., 2000, NESJE and DAHL, 2003; FEALY and SWEENEY, 2005), special focus is given to the construction of various circulation indices as predictors. The results of these analyses are described in chapter 4.

The second aim of this study is to use the statistical dependences between regional and large scale atmospheric variables and glacier mass balance to construct a dynamic statistical model for the generation of glacier mass balance estimates. Studies by NESJE et al. (1995), NESJE and DAHL (2003), NORDLI et al. (2005), NESJE (2005) and WATSON et al. (2006) demonstrate the success of the application of this principle for the reconstruction of glacier development. The results of the first investigation can be used to create such an estimate by applying the model output statistics (MOS) technique (GLAHN and LOWRY, 1972). This technique is common in modern weather forecasting, climatology and climate impact research (e.g. KRISHNAMURTI et al., 1999; LANDMAN and GODDARD, 2002; PAETH and HENSE, 2003; FRIEDRICHS and PAETH, 2006, PAETH et al. 2006, PAETH et al., 2008, PAETH, 2011). To ensure the robustness of this statistical model,

it is cross validated with independent data (MICHAELSEN, 1987). Such a model can directly be coupled to future climate simulations and takes regional disparities into consideration. Since it is not possible to give an a priori assessment of the correctness of predictions made by different climate model, the glacier mass balance estimates generated from them are presented as a multi-model ensemble. These estimates are presented in chapter 5.

The final aim is to address the question of which of the modelled climate future time periods is the most probable one given different observed states of the atmosphere in the past. Present-day atmospheric states favouring summer and winter mass balance minima and maxima are categorised into different time periods of modelled climate using a Bayesian classification approach (e.g. MIN et al., 2004; TEBALDI et al., 2005; PAETH et al., 2007). The resulting probabilities may aid in the interpretation of whether future climate favours particularly positive or negative mass changes in the different seasons. The results of this classification are presented in chapter 6.

2 Datasets

This chapter describes the datasets used in this study. Efforts were made to choose the most suitable and up-to-date datasets available at the time of the beginning of the study. The chapter is subdivided into a section on observational datasets, including glacial mass balance- and re-analysis data, and a section on the used climate model simulations. In addition to general descriptions of the datasets, comments on their suitability for this particular study are also provided.

2.1 Observational Datasets

The observational datasets are used to describe present day atmospheric- and glacial mass balance variability, to test for linear dependence between those, to construct the multiple regression model that can be used in combination with simulated future climate to produce estimates of future glacial mass balance changes. The observational datasets are also used to provide the data basis for the Bayesian assessment of probabilities of time periods of modelled climate in view of present-day observations.

2.1.1 NVE Glacier Mass Balance

The Norwegian Water Resources and Energy Directorate (NVE) supports a mass balance program and provides mass balance measurements for various glaciers in Norway. In accordance with the stratigraphic method (ØSTREM and BRUGMAN, 1991), the mass balance is calculated using two successive summer surfaces, or surface minima, and therefore describes the state of the glacier at the end of melting and before new snow accumulation. The net balance, as well as the summer balance, is obtained from stake measurements in September or October (ANDREASSEN et al.,

2011). The winter balance is obtained in April or May by probing to the summer surface of previous year along a profile that is kept approximately consistent throughout the years (ANDREASSEN et al., 2011). Stake measurements and snow coring is used in addition to probing (ANDREASSEN et al., 2011). Since the oldest mass balance measurements in 1949 on Storbreen, 42 additional glaciers have been subject to similar measurements (ANDREASSEN et al., 2011). Since 1963, six glaciers in southern Norway have been measured continuously (ANDREASSEN et al., 2011). Practical and methodical limitations, such as the inability to identify the exact time of the shift from the melting- to the accumulation period and the inability conduct measurements at that time, may results in inaccuracies such as an attribution of summer season mass loss to the winter season accumulation and thus in an underestimation of both summer melting and winter accumulation (ANDREASSEN et al., 2011).

The methods applied in this study (section 3) require long records of mass balance to ensure the reliability and significance of the results. Therefore, glaciers with fewer than 20 years of measurements were not given further consideration. Figure 2.1 shows the location of all the glaciers used in this study. Those with records of 20-30 years (Figure 2.1, grey), i.e. Austdalsbreen, Hansebreen and Langfjordjøkelen, were given limited consideration. The remaining, more suitable glaciers (Figure 2.1, colour coded) include Ålfotbreen, Nigardsbreen, Hardangerjøkelen, Storbreen, Hellstugubreen and Gråsubreen in South Norway, and Engabreen in the North. The southern glaciers lie on a similar latitude and have a different distance to the shoreline, making them ideal for the investigation of the effects of different degrees of continentality on the nature of the glaciers' interactions with climate.

In this study, the bi-annual NVE mass balance records of the mentioned glaciers are used to test for a linear dependence with several atmospheric variables, and serve as predictands in the multiple linear regression procedure. Ultimately, they are used to determine the composites of years of minimum, average and maximum mass balance in the Bayesian assessment of probabilities of time periods of modelled climate.

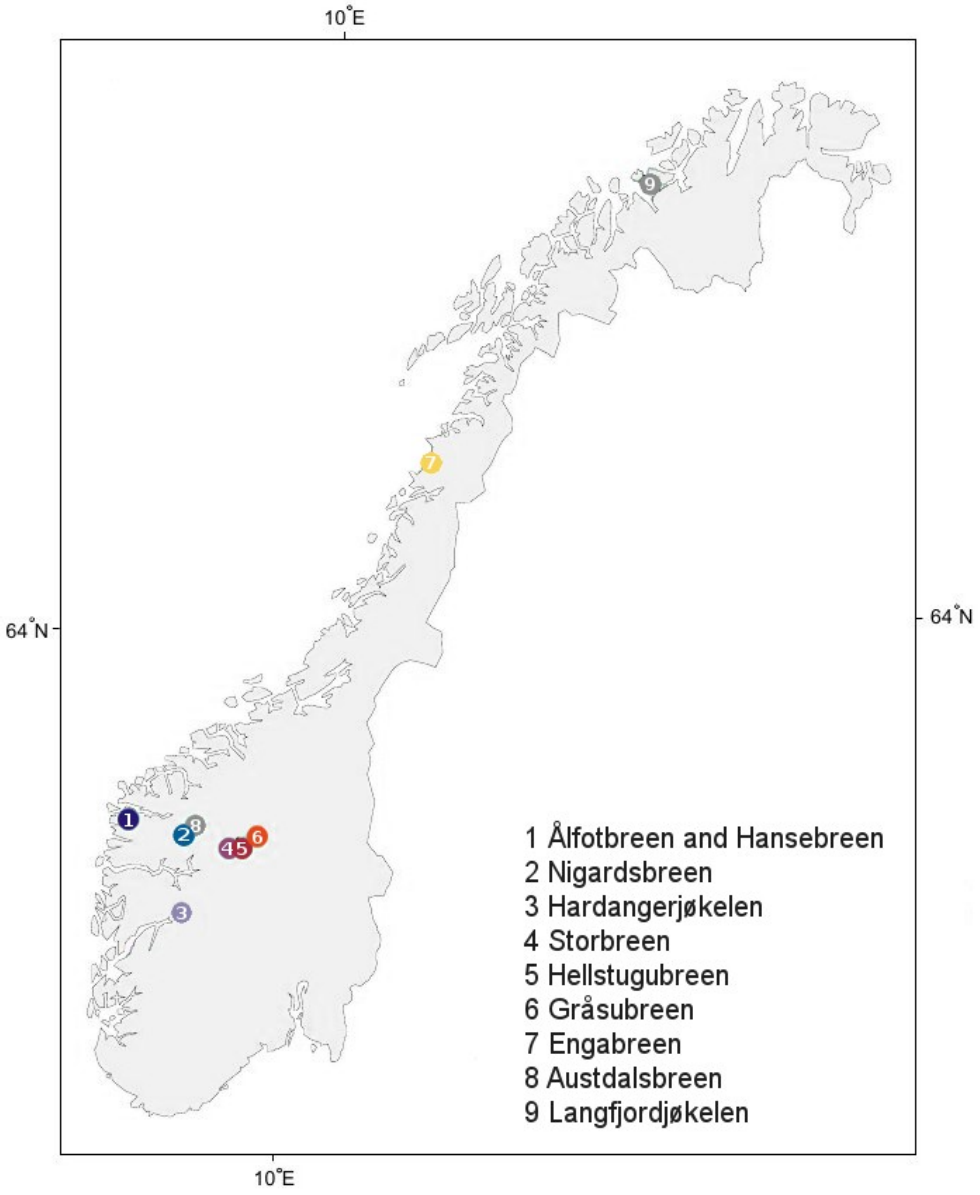

Figure 2.1: Location of glaciers used in this study, incl. glaciers given limited consideration (grey) and glaciers used in the multiple regression model (color coded), modified following ANDREASSEN et al., 2011.

2.1.2 NCEP/NCAR and ERA40 Re-analyses

The re-analyses of the National Centers for Environmental Prediction/National Center for Atmospheric Research (NCEP/NCAR) are constructed from recovered land surface, ship, satellite, aircraft, rawinsondes and other observational data, and dynamically interpolated with an operational forecast model to produce a more homogeneous, global

dataset (KALNAY et al., 1996; KISTLER et al., 2001). The forecast model has a spectral horizontal T62 resolution and 28 vertical levels (KALNAY et al., 1996). Quality controls and the data assimilation system were kept identical during the reanalysis project in order to avoid unnecessary inconsistencies, such as perceived jumps in climate (KALNAY et al., 1996). The problem of further possible inhomogeneities caused by changes in the observing systems was addressed by implementing parallel re-analyses with and without the use of the new observing system for at least one year following its introduction (KALNAY et al., 1996). The re-analysis product itself consists of global, gridded, daily and monthly values of several atmospheric variables at different pressure levels, covering a time range from 1948 until today (NCEP/NCAR, EARTH SYSTEM RESEARCH LABORATORY, 2011).

The ERA40 re-analysis of the European Centre for Medium-Range Weather Forecasts (ECMWF) was constructed from 40 years of meteorological observations from satellites, aircrafts, ocean-buoys, other surface platforms and radiosondes (UPPALA et al., 2005). The data assimilation system of the project improved upon the first generation system of the ERA15 re-analysis project (GIBSON et al., 1997) and previous NCEP/NCAR re-analyses, providing a horizontal spectral T159 resolution and 60 vertical levels (UPPALA et al., 2005). The re-analysis product consists of global, gridded, daily and monthly values of several variables at different vertical levels, covering a time range from mid-1957 to mid-2002 (ECMWF, 2012).

The time range of glaciological datasets (section 2.1.1) is only partially covered by the ERA40 re-analysis and fully covered by the NCEP/NCAR re-analysis. Since the possible shift in the glaciological regime in the late 1980's (section 1.1) is considered in this study, the temporal overlap of atmospheric data and mass balance records before and after the regime shift ought to be sufficiently large for the methods applied here. This makes the NCEP/NCAR re-analysis data the more suitable. Therefore, this dataset is used to determine seasonal variability of surface temperature and precipitation rate of mid-latitude Norway, and to calculate the seasonal variability of northern hemisphere circulation from sea level pressure. The resulting variables are then used to test for a linear dependence with

glacial mass balance and serve as predictors in the multiple linear regression procedure. Finally, they used as a basis for the Bayesian assessment of probabilities of modelled future climate time periods. The ERA40 dataset is used to construct the same variables. In the same fashion, these are then used to test for a linear dependence with glacial mass balance. The results of it serve as a cross reference for the results obtained using the variables constructed from NCEP/NCAR re-analyses.

2.2 CMIP3 Climate Model Dataset

The World Climate Research Programme's (WCRP's) Coupled Model Intercomparison Project phase 3 (CMIP3) multi-model dataset (MEEHL et al. 2007) is used for the reconstruction of climate predictors, which are in turn used with the multiple regression models to generate estimates for present-day and future glacier mass balance (section 3.4). It is an archive of climate model simulation output from over 20 climate models that are included in the fourth IPCC assessment report (2007). In addition to natural climate variability, external forcings such as the increase in atmospheric greenhouse gases, can be defined for simulations of future climate in order to model the sensitivity of climate to these forcings (VON STORCH et al., 1999; CUBASCH and KASANG, 2000). The different emission scenarios for anthropogenic greenhouse gases describe different scenarios for the future development of demographics, society, economy and technology (NAKICENOVIC, 2000; NAKICENOVIC and SWART, 2000). The frequently used B1, A1b and A2 scenarios assume atmospheric CO_2 concentrations of 550, 700 and 850 ppm in 2100 respectively (GIORGI and COPPOLA, 2009).

Model (CMIP I.D.)	Country	Associated Research Group(s)
BCCR-BCM2.0	Norway	Bjerknes Centre for Climate Research
CCM3	USA	National Center for Atmospheric Research
CGCM3.1(T63)	Canada	Canadian Centre for Climate Modelling & Analysis
CNRM-CM3	France	Météo-France / Centre National de Recherches Météorologiques
CSIRO-Mk3.0	Australia	CSIRO Atmospheric Research
CSIRO-Mk3.5	Australia	CSIRO Atmospheric Research
ECHAM4/MPI-OM	Germany	Max Planck Institute for Meteorology
ECHAM5/MPI-OM	Germany	Max Planck Institute for Meteorology
GFDL-CM2.0	USA	US Dept. of Commerce / NOAA / Geophysical Fluid Dynamics Laboratory
GFDL-CM2.1	USA	US Dept. of Commerce / NOAA / Geophysical Fluid Dynamics Laboratory
INM-CM3.0	Russia	Institute for Numerical Mathematics
IPSL-CM4	France	Institut Pierre Simon Laplace
MIROC3.2(hires)	Japan	Center for Climate System Research National Institute for Environmental Studies, and for Global Change (JAMSTEC)
MIROC3.2(medres)	Japan	Center for Climate System Research National Institute for Environmental Studies, and for Global Change (JAMSTEC)
MRI-CGCM2.3.2	Japan	Meteorological Research Institute
PCM	USA	National Center for Atmospheric Research
UKMO-HadCM3	UK	Hadley Centre for Climate Prediction and Research / Met Office
UKMO-HadGEM1	UK	Hadley Centre for Climate Prediction and Research / Met Office

Table 1: List of included climate models from the CMIP archive, showing the model CMIP ID (left), and associated country (centre) and research group (right).

The CMIP3 dataset includes output from 1-7 individual climate model runs per scenario. The available scenarios include a 20th century scenario (20c3m) and the three future scenarios B1, A1b and A2. Several models in the CMIP3 dataset miss simulation results for one or more of the four scenarios. Other models have a very coarse resolution. In order to avoid bias in the estimates of the glacier mass balance estimates, these models were not used for the construction of predictors. The remaining 18 models are listed in table 1.

3 Applied Methods

This chapter describes the methods applied in this study in the approximate chronological order of their execution. These include both basic and advanced tools in statistical climatology that are already established in scientific literature. The chapter is subdivided into sections describing the methods used for the analysis of glacial mass balance datasets, the construction of atmospheric variables from ERA40 and NCEP/NCAR re-analyses and from CMIP3 climate model simulations, the correlation analysis between observed glacial mass balance and each of the constructed atmospheric variables, the stepwise multiple linear regression, the generation of glacial mass balance estimates with aid of the multiple regression model and atmospheric variables constructed from the CMIP3 dataset, and the Bayesian classification of present-day atmospheric states into different time periods of modelled climate. Each section provides a short introduction and justification for the methods used, a description of the procedure, and a depiction of how the methods are applied in this particular study. Further explanations are provided for deviations from procedures in published literature, as well as for study-specific parametrisations.

3.1 Preparation of Glacier Mass Balance Data

This section outlines the methods used for the preparation of the NVE glacier mass balance data. Winter and summer mass balances are treated separately throughout the entire study and only combined to calculate the final net mass balance estimates. The data from the bi-annual measurements carried out as part of the NVE glacial mass balance program (section 2.1) is provided in the desired format as total winter and

summer mass balances representing the total mass loss during the melting season between April or May and September or October, and the total mass gain during the accumulation season between September or October and April or May. However, since temporal autocorrelation, i.e. the internal stochastic dependences between temporally neighbouring values, would violate the statistical assumptions of regression and might induce biases in interpretations of the regression results, the mass balance times series are tested for such dependences prior to the correlation and regression analyses involving the atmospheric variables (section 3.3 and section 3.4). To ensure temporal homogeneity of mean and variance, the linear trend is removed before the autocorrelation analysis. The investigated stochastic dependence between the values of variable $X = x(t_1), x(t_2), \ldots, x(t_n)$ at different times can be expressed as a function of the number of discrete time steps τ, by which variable X is temporally shifted against itself. This results in variables $X[\tau] = x(t_1), x(t_2), \ldots, x(t_{n-\tau})$ and $X(\tau) = x(t_{1+\tau}), x(t_{2+\tau}), \ldots, x(t_n)$, where n is the original sample size. The number of samples available for the calculation of $r(\tau)$, describing the dependence between the resulting variables $X[\tau]$ and $X(\tau)$, consequently decreases from $n-1$ at $\tau=1$ to zero at $\tau=n$. The measure of dependence $r(\tau)$ is usually estimated as the Pearson correlation coefficient between $X[\tau]$ and $X(\tau)$ (BAHRENBERG et al., 1999; SCHÖNWIESE, 2006), so that $-1 \leq r(\tau) \leq 1$ and

$$r(\tau) = \frac{cov(X[\tau], X(\tau))}{\sqrt{var(X[\tau]) \cdot var(X(\tau))}}$$

The significance of the autocorrelation function is calculated for each time step by testing the null hypothesis $H_0 : \rho(\tau) = 0$, which states that no autocorrelation exists. The test statistic

$$g(\tau) = \left| \frac{r(\tau)}{\sigma_{r(\tau)}} \right|$$

is approximately standard normally distributed, so that the significance can be determined in the usual manner from the standard error $\sigma_{r(\tau)}$ (BAHRENBERG et al., 1999; SCHÖNWIESE, 2006):

$$\sigma_{r(\tau)} = \frac{\sqrt{1+2\cdot\sum_{j=1}^{\tau-1} r(j)^2}}{\sqrt{n}}$$

In the 2-tailed test of this study, the critical value for the test statistic is 1.65, which translates to a significance level of 10%. If the estimated value lies outside this interval, the null hypothesis is rejected and the alternative hypothesis $H_A : \rho(\tau) \neq 0$ is accepted. The calculations are carried out for $\tau = t_1, t_2, .., t_n$ and results are presented as the number of instances of τ,for which autocorrelation prevails in succession.

3.2 Construction of Atmospheric Variables

This section describes the methods used for the construction of atmospheric variables that are likely to show dependences with the glacier mass balance time series or have been shown to correlate with glacier mass balance in previous studies. They are constructed from the NCEP/NCAR and ERA40 re-analyses and later used correlation analyses (section 3.3) to create a pre-selection of atmospheric variables for the multiple regression (section 3.4). After the multiple regression analyses have been carried out and the most important predictors have been identified, these variables are reconstructed from the CMIP3 climate model data, which is interpolated to the resolution of the NCEP/NCAR re-analysis data beforehand. Ultimately, the multiple regression model is applied to the reconstructed variables to generate an estimate for present-day and future glacial mass balance. Given that local meteorological time series from measurements in the vicinity of the glaciers often are not as well in phase with the glacial mass changes as larger scale atmospheric factors because many of the South-Norwegian glaciers are controlled by winter accumulation rather than summer air temperature changes (e.g. NESJE and DAHL, 2003; WINKLER and NESJE, 2009), special focus is given to the contruction of atmospheric circulation indices.

3.2.1 Spatiotemporal Means

Temperature and precipitation, the most important direct controls of ablation and accumulation, are included as spatiotemporal arithmetic means of the respective NCEP/NCAR and ERA40 re-analysis variables. 2m air temperatures and precipitation rates are averaged over different sets of months for each of the re-analysis fields. Analogous to the seasons used for the construction of variables in section 3.2.2 and 3.2.3, the data is averaged over months DJF, MAM, JJA and SON. In consideration of the glaciological seasons of ablation and accumulation (section 2.1.1), the year is also subdivided into the six months seasonal means AMJJAS and ONDJFM. The temporal means are then averaged over southern Scandinavia. Since the majority of investigated glaciers are in South-Norway, and to avoid the inclusion of possibly more irrelevant northern temperature and precipitation, only the fields up to a latitude of approximately 66° are taken into account. The result is a time series for each of the sets of seasons. The spatiotemporal means used in the multiple regression model (section 3.4) are then reconstructed from the corresponding temperature and precipitation variables of the CMIP3 dataset. They calculated for each scenario, model and model run separately.

3.2.2 Stationary NAO Indices

The North Atlantic Oscillation (NAO) can be described as the movement of atmospheric mass between Arctic and subtropical latitudes across the North Atlantic (TEISSERENC DE BORT, 1883; WALKER, 1924), and has previously been used to explain variations in glacial winter mass balance (section 1.1, e.g. NESJE and DAHL, 2003; FEALY and SWEENEY, 2005; CHINN et al., 2005.). The NAO variability can be quantified in several ways as different indices and derived from atmospheric pressure. Stationary NAO indices are obtained from differences between standardised monthly or seasonal surface pressures at specific, fixed locations in Iceland and the Azores (e.g. HURRELL, 1995). The coordinates are based on the locations of meteorological stations. Even though the NCEP/NCAR and ERA40 datasets do not impose the same geographical limitations in the choice of

coordinates, this study adheres to the published, conventional pairs of locations. The three stationary NAO indices that are constructed in this study are the Ponta Delgada-Reykjavik, the Lissabon-Reykjavik (HURREL, 1995,) and the Gibraltar-Reykjavik (JONES et al. 1997) index. For each year, and at each location separately, seasonal (in this case DJF, JJA) means of NCEP/NCAR and ERA40 sea level pressure values are constructed. The variability of atmospheric pressure pattern is described by the difference of normalised seasonal mean sea level pressure between the two locations. To obtain the index values, the Iceland anomaly is subtracted from the Azores anomaly. The inherent problem of using sea pressure at fixed locations is the unlikeliness that the NAO's centres of action are located exactly at these coordinates. Consequently, the maximum pressure gradient cannot be captured. Section 3.2.3 includes a description of the construction of a dynamic NAO index time series by means of a principal component analysis (NOAA-CPC, 2012).

3.2.3 Principal Component Analysis

The Principal Component Analysis (PCA), or Empirical Orthogonal Functions (EOF), is a multivariate statistical tool that allows the reduction of the dimensions of a dataset with multiple correlated variables to fewer groups of variables with similar variation. These factors, or principal components, are stochastically independent and orthogonal to each other. Unlike the factor analysis, the PCA assumes that the variance of the original dataset can be reproduced by a linear combination of all principal components and their respective eigenvectors (e.g. BAHRENBERG et al., 2008; VON STORCH and ZWIERS, 1999; WILKS, 2006). The reduced dimension of the original dataset can represent the number of different natural variables, as well as different geographical locations of the same variable. In the latter case, the PCA produces spatial patterns describing the centres of variation of each principal component (VON STORCH and ZWIERS, 1999).

Given the *n* x *m* dimensional data matrix *X* as a starting point, where *n* are the spatial units $R_1, R_2, \ldots, R_n$ and *m* are the reference units of time $T_1, T_2, \ldots, T_m$, x_{ij} is the value of R_i at the time unit T_j. The data anomaly

matrix X' is constructed by subtraction of the temporal means $\bar{x}_i$ from x_{ij}. In order to identify the spatial patterns of centres with similar variation, i.e. modes of variations (JACOBEIT et al., 1998; VON STORCH and ZWIERS, 1999), the n x n dimensional covariance matrix C is constructed as:

$$C = \frac{1}{m-1} \cdot X'^{T} \cdot X'$$

Unlike a correlation matrix, the covariance matrix does not assign equal weightings to all spatial units (VON STORCH and ZWIERS, 1999). The covariance matrix is then used to determine the n x n dimensional eigenvector matrix E and the diagonal matrix Λ, storing the n corresponding eigenvalues (VON STORCH and ZWIERS, 1999; WILKS, 2006) so that:

$$C = E \cdot \Lambda \cdot E^{T}$$

In the n-dimensional coordinate space, the first eigenvector is directed at the maximum variance of the matrix X', and the subsequent eigenvectors oriented orthogonally to it and the other eigenvectors, creating the axes of a new coordinate system for X'. The loadings, i.e. the spatial patterns associated with each eigenvector, can be interpreted as the geographical fields of the investigated variable that contribute to the formation of the corresponding principal component. Therefore, they also represent the geographical pattern of similar variations within X' (VON STORCH and ZWIERS, 1999; WILKS, 2006). The matrix of principal components is obtained from the projection of X' onto E (VON STORCH and ZWIERS, 1999; WILKS, 2006). The scores, i.e. the n components of the matrix forming time series of length m, describe the common change of the spatial units of the associated eigenvectors over time. Since the sum of the eigenvalues λ_i of the n principal components make up the total variance of X', the variance R_k of X' explained by the k^{th} principal component can be calculated as (VON STORCH and ZWIERS, 1999; WILKS, 2006):

$$R_k = \frac{\lambda_k}{\sum_{i=1}^{n} \lambda_i}$$

The principal components are sorted in descending order by the amount of variance of X' they explain.

In this study, the PCA is carried out for different time spans and fields of sea level pressure, and combined sea level pressure, temperature and precipitation. Since this study is carried out with particular consideration of the possible shift in the glaciological regime of the investigated glaciers (section 2.1), and the ERA40 dataset covers less of the time periods marked by these different regimes (section 2.2), the atmospheric variables used in the multiple regression are constructed from the NCEP/NCAR dataset. Since the loading patterns of the principal components vary depending on the investigated time period, all the principal component analyses described in this section are carried out for the time periods 1949-1988 and 1989-2008, in which the different glaciological regimes may prevail, as well as for the total time span from 1949 to 2008. Two different fields of seasonally averaged sea level pressure are used in the principal component analyses that are carried out with the aim to describe modes of variation of atmospheric pressure. The PCA using sea level pressure north of 20° ought to generate an index time series for the Arctic Oscillation (AO) or Northern Annular Mode (NAM) as the first principal component (PC) (BARNSTON and LIVEZEY 1987, NOAA-CPC 2012), and is referred to as PCA_{NH} in this study. The first PC of the second PCA (PCA_{NA}) using a sea level pressure field over the North Atlantic, bounded by longitudes of 40° East and 90° West and latitudes of 20° and 80° North, can be used as an index time series for the NAO (NOAA-CPC 2012). In order to consider the difference in sizes of the spatial units in the PCA procedure, the sea level pressure anomalies are weighted by the square root of the cosine of the latitude.

The control of the NAO and AO on temperature and precipitation in Europe (NOAA-CPC 2012) leaves these variables highly correlated. To avoid possible multicollinearity related problems in the multiple regression analysis and in the interpretation of its results, another two principal component analyses are carried. The aim is to create a set of new uncorrelated variables that including the variability of temperature and precipitation as well as that of sea level pressure. Temperature and precipitation fields of dimension $n_2 \times m$ and $n_3 \times m$ respectively are used in combination with to the $n_1 \times m$ dimensional sea level pressure field. The

number of time steps m is consistent between the datasets, while the spacial units R_i may differ. The anomaly matrices A', B' and C' are constructed from data matrices A, B and C and combined to produce the anomaly matrix:

$$X' = \begin{pmatrix} a'_{11} & a'_{21} & \cdots & a'_{n_1 1} & b'_{11} & b'_{21} & \cdots & b'_{n_2 1} & c'_{11} & c'_{21} & \cdots & c'_{n_3 1} \\ a'_{12} & & & a'_{n_1 2} & & & & b'_{n_2 2} & & & & c'_{n_3 2} \\ \vdots & & & \vdots & & & & \vdots & & & & \vdots \\ a'_{1m} & a'_{2m} & \cdots & a'_{n_1 m} & b'_{1m} & b'_{2m} & \cdots & b'_{n_2 m} & c'_{1m} & c'_{2m} & \cdots & c'_{n_3 m} \end{pmatrix}$$

The loading patterns associated with the eigenvectors can be extracted and translated back to three separate geographic maps showing the spatial patterns of similar variations of sea level pressure, temperature and precipitation associated with one principal component. The first PCA (PCA$_{STP1}$) carried out in this way uses fields of equal sizes for all variables. This field corresponds to the field used for PCA$_{NA}$, and thus includes the temperature and precipitation variability over the North Atlantic. However, this might lead to the problem that the temperature and precipitation variability relevant to Norwegian glaciers might be overshadowed by the strong variability of these temperature and precipication over the North Atlantic. While the relevant variability ought still be included in the sum of all principal components, it might not be described by the leading PC or any particular few principal components, but distributed among them. Since this would require the inclusion of an undesirably great number of principal components and cause problems in the multiple regression (section 3.4), the second PCA (PCA$_{STP2}$) uses the same temperature and precipitation fields that are used for the spatiotemporal means (section 3.2.1).

3.3 Correlation Analysis

The linear dependence between each atmospheric variables and glacial mass balance is determined by the Pearson correlation coefficient (e.g. BAHRENBERG et al., 1999, SCHÖNWIESE 2006). Given the possible change in the glaciological regime, different climatic factors can change the strength and nature of their dependence with glacial mass. Therefore, as

well as using the entire temporal overlap between mass balance- and re-analysis data, moving 10 year periods of the time series are used in order to track time- or regime specific dependences. The correlation coefficient $r(\tau)$ is calculated for time shifts $\tau = 0, \ldots, n-10$, where τ represents the number of discrete time steps from the earliest common time step of the temporal overlap of atmospheric variable X and mass balance variable Y. Consequently, the correlation coefficient is calculated for time series $X(\tau) = x(t_{1+\tau}), x(t_{2+\tau}), \ldots, x(t_{10+\tau})$ and $Y(\tau) = y(t_{1+\tau}), y(t_{2+\tau}), \ldots, y(t_{10+\tau})$ for each τ, so that

$$r(\tau) = \frac{cov(X(\tau), Y(\tau))}{\sigma_{X(\tau)} \cdot \sigma_{Y(\tau)}}$$

The significance of $r(\tau)$ is determined in a similar way as in section 3.1, but the critical value for the test statistic is more strict and resulting significance levels are binned into <0.01, 0.01-0.05 and 0.05-0.1 for the presentation of results in section 4.2 while the correlation coefficients below the 0.1 level are considered insignificant. In addition to giving insight into linear dependences and possible changes in them over time, the correlation analyses between atmospheric variables and glacial mass balance also serve as a discrimination procedure to help construct a pre-selection of atmospheric variables that are used as predictors in the multiple regression.

3.4 Multiple Regression Analysis and Prediction

The multiple linear regression relates several independent variables, known as predictors, to a dependent variable, known as the predictand. It can serve as a tool for the investigation of the influence of the predictors on the predictand, or to produce an estimate for the predictand with the aid of a set of predictors and regression coefficients. The multiple linear regression is based on the simple linear regression, but includes multiple independent variable (e.g. BAHRENBERG et al., 2008; VON STORCH and ZWIERS, 1999; WILKS, 2006). In this study, a multiple regression is performed to assess the influence of several climate related predictors on glacial mass balance, and to generate an estimate for glacial mass changes.

The predictors are constructed from NCEP/NCAR re-analysis data as described in section 3.2 and pre-selected as described in section 3.3. The NVE glacial mass balance time series are used as predictands without further modification if they do not show any significant autocorrelation (section 3.1). The resulting multiple regression model is then applied to the climate predictors reconstructed from the CMIP3 model dataset to generate an estimate for present-day and future glacial mass changes. The temporal overlap of estimated and observed present-day glacial mass balance allows a calibration of the estimates.

Before the analysis, the data series are standardised. The cross-validated stepwise multiple linear regression itself is an adjustment of the procedures described by PAETH and HENSE (2003) and PAETH et al. (2006) to the problem addressed in this study. It is set up as follows: The included predictors are sorted by their importance, which is determined by linear regression analyses between the n dimensional predictand time series $\vec{y}$ and the predictor time series $\vec{x}_1, \ldots, \vec{x}_k$ (VON STORCH and ZWIERS 1999). The most important predictor, as determined by the strength of its relationship with the predictand, is selected for the regression analysis and the residual $\vec{\varepsilon}$ is calculated. The residual is then used in regression analysis with the subsequent predictor and a new residual is determined. This method is continued with all predictors included in the multiple regression model. For cross-validation following MICHAELSEN (1987) and VON STORCH and ZWIERS (1999), a reasonable number of values, usually between five and eight, is retained before each regression analysis. The regression model is trained with the dependent data, i.e. the data left after the removal of the randomly selected bootstrap values. The model is then applied to the retained data and the root mean square error (RMSE) between the independent predictand data and regression model estimates is calculated. Once the RMSE ceases to decrease, the currently used predictor is not included in the model and the multiple regression is terminated. This results in an exclusion of predictors that do not provide any additional information about the independent data. The whole process is repeated 1000 times. Each time, a different set of bootstrap values is retained and the resulting regression equation is saved. The coefficients

are averaged over all iterations for the final model. To ensure the robustness of the model, a filter for predictors is introduced before the computation of the final multiple regression. Only predictors that pass through the filter in at least 50% of all iterations are included in the final model. The described procedure prevents an overfitting of the model, but multicollinearity causes predictors to compete for the inclusion into the model. For that reason, the highly correlated predictors calculated in PCANA and PCANH (section 3.2.3) are placed in separate predictor sets along with temperature and precipitation. The multiple regression is also carried out for the uncorrelated 12 leading principal components of PCASTP1 and PCASTP2, resulting in a total of 4 different predictor sets. Since the retaining of bootstrap values shortens the model training period, only glaciers with sufficiently long times series are included in the model (section 2.1.1). In order to take into account the possible shift in the glaciological regime (section 1.1), the time periods 1949-1988, 1989-2008 and 1949-2008 are considered separately. The cross-validated stepwise multiple linear regression is performed for each glacier, season, time period and predictor set. For each,

$$y_i = \varepsilon_i + a + \sum_{j=1}^{k} b_j \cdot x_{ij} \,,$$

where $\vec{y} = \begin{pmatrix} y_1 \\ \vdots \\ y_n \end{pmatrix}$; $\boldsymbol{X} = \begin{pmatrix} x_{11} & x_{21} & \cdots & x_{k1} \\ x_{12} & & & x_{k2} \\ \vdots & & & \vdots \\ x_{1k} & x_{2k} & \cdots & x_{kn} \end{pmatrix}$; $\vec{b} = \begin{pmatrix} b_1 \\ \vdots \\ b_k \end{pmatrix}$; $\vec{\varepsilon} = \begin{pmatrix} \varepsilon_1 \\ \vdots \\ \varepsilon_n \end{pmatrix}$,

ε_i is the residual, a is the y-axis intercept and $b_1, \ldots, b_k$ are the regression coefficients for corresponding $\vec{x}_1, \ldots, \vec{x}_k$, n is the number of predictands, i.e. summer and winter mass balance time series for each glacier included in the model, and k is the number of predictors in the predictor sets.

The estimates $\hat{y}_1, \ldots, \hat{y}_n$ are generated from (e.g. BAHRENBERG et al. 2008):

$$\hat{y}_i = a + \sum_{j=1}^{k} b_j \cdot x_{ij} \,,$$

where the predictors $\vec{x}_1, \ldots, \vec{x}_k$ created from the NCEP/NCAR dataset are substituted by the corresponding predictors recreated from the CMIP3

model dataset (section 3.2). This point estimate can be complemented by an interval estimate, so that (e.g. BAHRENBERG et al., 2008):

$$\hat{y}_i - S_{B_{01...k}} \leq y_i \leq \hat{y}_i + S_{B_{01...k}} ,$$

where the $S_{B_{01...k}}$ is the standard error of y_i, i.e. the standard deviation of the residual ε_i. These estimates are generated for each climate model, scenario and run separately. Since the means of the calculated estimates are unknown, the model output needs to be calibrated. The mean for each of the present-day 20c3m scenario $\hat{y}_i$ estimates is adjusted to the known mean of the observed y_i in the overlapping time period. For the short temporal overlap of the 20c3m and the future scenario estimates, the means of the future estimates are adjusted to the 20c3m mean in the same fashion. This is carried out for each individual run and model. The estimates are then averaged over the different model runs to create model ensemble means. In order to avoid bias induced by different numbers of runs per model scenario, the multi-model means are constructed by averaging the ensemble means over the different models. This is done for the present-day estimates and the future estimates for the time period covered by all runs. This results in estimates for years 1950-2100.

3.5 Bayesian Classification Procedure

One of the questions addressed in this study is whether the observed states of the atmosphere at particular times can be classified into a past, imminent or distant future of modelled climate. Bayesian statistics offers the tools for such a classification (BERGER 1985; LEROY 1998; BERLINER et al. 2000; MIN et al. 2004; TEBALDI et al. 2005; PAETH et al. 2007). In stochastic terms, the problem can be expressed as an investigation of which of these time periods $m_i, i = 1,...,n$ is the most probable one given the observed state of the atmosphere $\boldsymbol{d}$ at time t (e.g. MIN et al., 2004; PAETH et al., 2007). The state of the atmosphere is described by a set of k variables, making $\boldsymbol{d}$ a k-dimensional vector. In accordance with the Bayes theorem, the likelihood $p(\boldsymbol{d}|m_i)$ relates the prior probabilities $p(m_i)$ to the

posterior probabilities $p(m_i|\boldsymbol{d})$ such that (e.g. LEROY, 1998; Berliner et al. 2000; SIVIA and SKILLING, 2006; PAETH et al., 2007):

$$p(m_i|\boldsymbol{d}, I) = \frac{p(\boldsymbol{d}|m_i, I) \cdot p(m_i|I)}{p(\boldsymbol{d}|I)}$$

Since there is no absolute probability, all probabilities are conditional on I, denoting the relevant background information under which the probability relations are valid (D'AGOSTINI, 2003; SIVIA and SKILLING, 2006). For reasons of readability, it is no longer be mentioned hereafter. The prior probability $p(m_i)$ represents the state of knowledge or ignorance before the analysis of observed data, while the posterior $p(m_i|\boldsymbol{d})$ represents the state of knowledge in view of the observations and is modified through the likelihood of the observations (e.g. BERGER, 1985; HASSELMANN, 1998). $p(\boldsymbol{d})$ acts as a normalising factor for the posterior probabilities and is calculated by

$$p(\boldsymbol{d}) = \sum_{i=1}^{n} p(\boldsymbol{d}|m_i) \cdot p(m_i) \, .$$

The likelihood is obtained by integration of the likelihood function, describing the probability of observing the atmospheric state $\boldsymbol{d}$ given the modelled atmospheric conditions that prevail in the different time periods, and the marginal probability density describing the probability of a specific realisation $\boldsymbol{f}$, which is also a k-dimensional vector, for the time period category, so that

$$p(\boldsymbol{d}|m_i) = \int p(\boldsymbol{d}|\boldsymbol{f}) \, p(\boldsymbol{f}|m_i) \, d\boldsymbol{f} \, .$$

It is assumed that the observed and modelled states of the atmosphere follow a multivariate Gaussian distribution. Thus the likelihoods are calculated via the mean vectors for the categories, the data vectors and covariance matrices (e.g. MIN et al. 2004).

The k-dimensional vectors describing the state of the atmosphere are defined by the variables used as predictors in the final multiple regression model for the generation of glacier mass balance estimates. The time period for which the estimates are generated, i.e. 1950-2100, is divided into five 30 year time periods to serve as the categories $m_i, i = 1, \ldots n$ for the classification procedure so that $n = 5$. Since it is not possible to give an a

priori estimate for $p(m_i)$, the probability is equally distributed among the time period categories. Winter and summer seasons are treated separately in the entire procedure. The analysis is carried out for each observational year in order to track the change in posterior probabilities for time periods of modelled atmospheric states as the observed atmospheric state changes in the latter half of the 20th century. In addition to the calculations done for single years of observations, the investigation is also carried out for composites of years. The selection of years that make up these composites relates this investigation to glacier mass balance. The years of most negative and most positive glacier mass balance are identified for each season and glacier separately. For all of the composites of years characterised by maxima and minima in mass balance, the temporally corresponding observed atmospheric states are averaged over the identified years. These arithmetic means are then used to construct the data vector $\boldsymbol{d}$ for the described Bayesian classification procedure. In order to track the sensitivity of posteriors to the number of years used in the construction of the composites, this number is varied between 3, 5 and 10.

4 Relationship Between Mid-Latitude Atmospheric Variability and Glacier Mass Balance

This chapter presents the results of the investigation into the present-day relationships between mid-latitude atmospheric variability and glacier mass balance. It is subdivided into a description of the nature of the mass balance variability, the variability of the constructed atmospheric variables (section 3.2), the stochastic dependence between these variables and the glacial mass balance as calculated in correlation analyses (section 3.3), and the results of the multiple regression analyses (section 3.4). For reasons of readability, the focus of the detailed descriptions lies on the atmospheric variables showing the strongest stochastic dependences with mass balance, and on those used in the multiple regression. This chapter only treats present-day conditions. The predictions made with the multiple regression model are presented in chapter 5.

4.1 Present-Day Mid-Latitude Atmospheric Variability

In this section the atmospheric variables constructed from NCEP/NCAR and ERA40 re-analyses are described. Special focus is given to the atmospheric variables showing a strong stochastic dependence with glacial mass balance, and those included in the multiple regression analyses.

4.1.1 Variability of North Atlantic Sea Level Pressure

The results of PCAna describe the variability of NCEP/NCAR North Atlantic seasonal sea level pressure anomalies over the area extending from 20°N to 80°N and from 90°W to 40°E. The five leading principal components of each, representing the most important modes of variation, are considered as predictors in the multiple regression analyses.

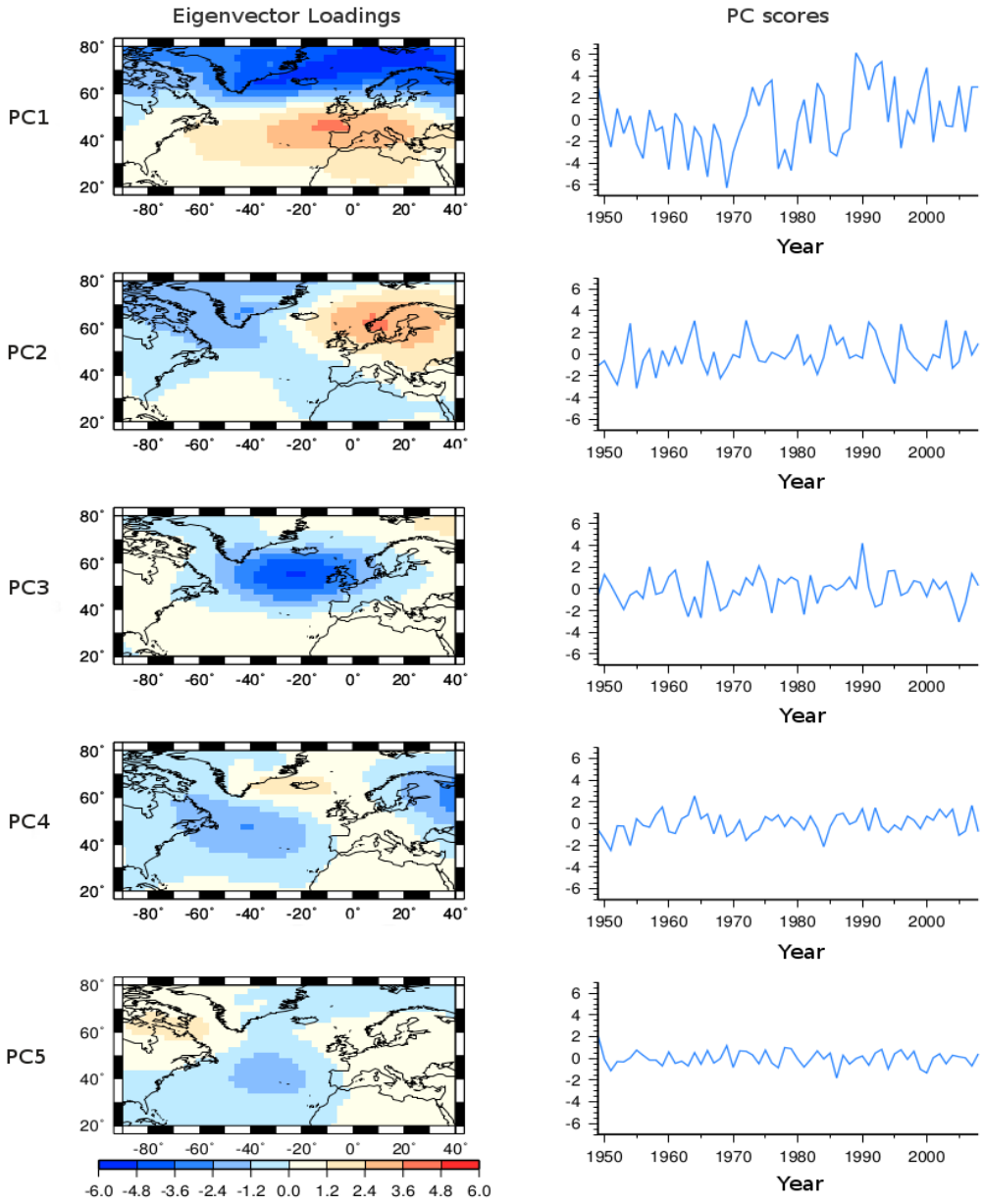

Figure 4.1: Eigenvector loadings (left) and PC scores (right) of the leading five PCs of PCAna.

Figure 4.1 shows the five leading PCs of the PCA$_{NA}$ using NCEP/NCAR winter (DJF) sea level pressure anomalies from 1949-2008. The first PC explains approximately half of the total variance of the sea level pressure anomalies in the said field. The eigenvector loadings first PC are characterised by one centre of variation over Iceland and the Norwegian Sea and a centre of variation with an opposite sign over the Bay of Biscay. These are consistent with the pressure anomalies associated with the North Atlantic Oscillation (NAO) (BARNSTON and LIVEZEY, 1987; NOAA-CPC, 2012). The second and third PC closely resemble Scandinavia Pattern (SCAND) (BARNSTON and LIVEZEY, 1987; NOAA-CPC, 2012) and the East Atlantic pattern (EA)(BARNSTON and LIVEZEY, 1987; NOAA-CPC, 2012) respectively. The nature of the fourth and fifth PC do not allow a confident identification when placed in context of the circulation patterns described in BARNSTON and LIVEZEY (1987). The first PC of the PCA$_{NA}$ using NCEP/NCAR summer (JJA) sea level pressure anomalies from 1949-2008 resemble the NAO summer pattern (NOAA-CPC, 2012). When PCA$_{NA}$ is carried out for different time periods, the PC scores and centres of action described by the eigenvector loadings change slightly, but are still identified as the same teleconnection patterns.

4.1.2 Variability of Northern Hemisphere Sea Level Pressure

The results of PCA$_{NH}$ describe the variability of NCEP/NCAR Northern Hemisphere seasonal sea level pressure anomalies over the area extending from 20°N to 90°N. The five leading principal components of each (Fig. 4.2), representing the most important modes of variation, are considered as predictors in the multiple regression analyses. When using NOAA-CPC (2012) and BARNSTON and LIVEZEY (1987) as a reference, the first, second, third and fifth PC of the PCA$_{NH}$ using NCEP/NCAR winter (DJF) sea level pressure anomalies from 1949-2008 can be identified as the Arctic Oscillation (AO) or Northern Annular Mode (NAM), the Pacific North American pattern (PNA), East Atlantic/Western Russia pattern (EA/WR) and the East Atlantic pattern (EA) respectively. The first and second PC of the PCA$_{NH}$ using NCEP/NCAR summer (JJA) sea level pressure anomalies from 1949-2008 identify as the summer NAM and the single centre Asian

summer pattern. When PCANH is carried out for different time periods, the PC scores and centres of action described by the eigenvector loadings change slightly, but still identify as the same teleconnection patterns.

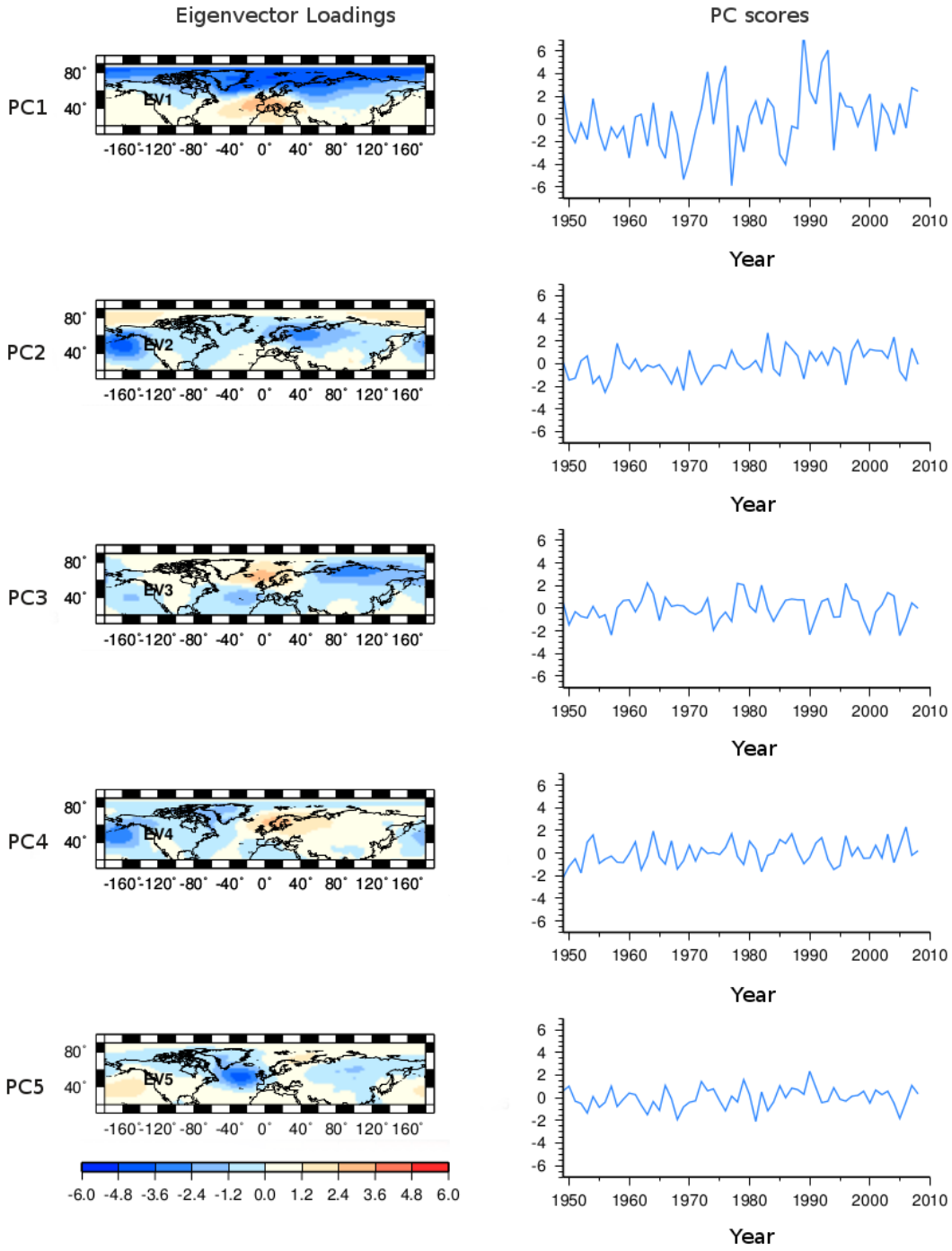

Figure 4.2: Eigenvector loadings (left) and PC scores (right) of the leading five PCs of PCANH.

4.1.3 Variability of Northern Hemisphere Sea Level Pressure, Temperature and Precipitation

The results of PCAstp1 and PCAstp2 describe the variability of NCEP/NCAR seasonal sea level pressure, temperature and precipitation anomalies. The sea level pressure field for both PCAstp1 and PCAstp2 extends from 20°N to 80°N and from 90°W to 40°E. In PCAstp1, the precipitation and temperature fields cover the same area, while in PCAstp2, they are restricted to an area covering southern Scandinavia.

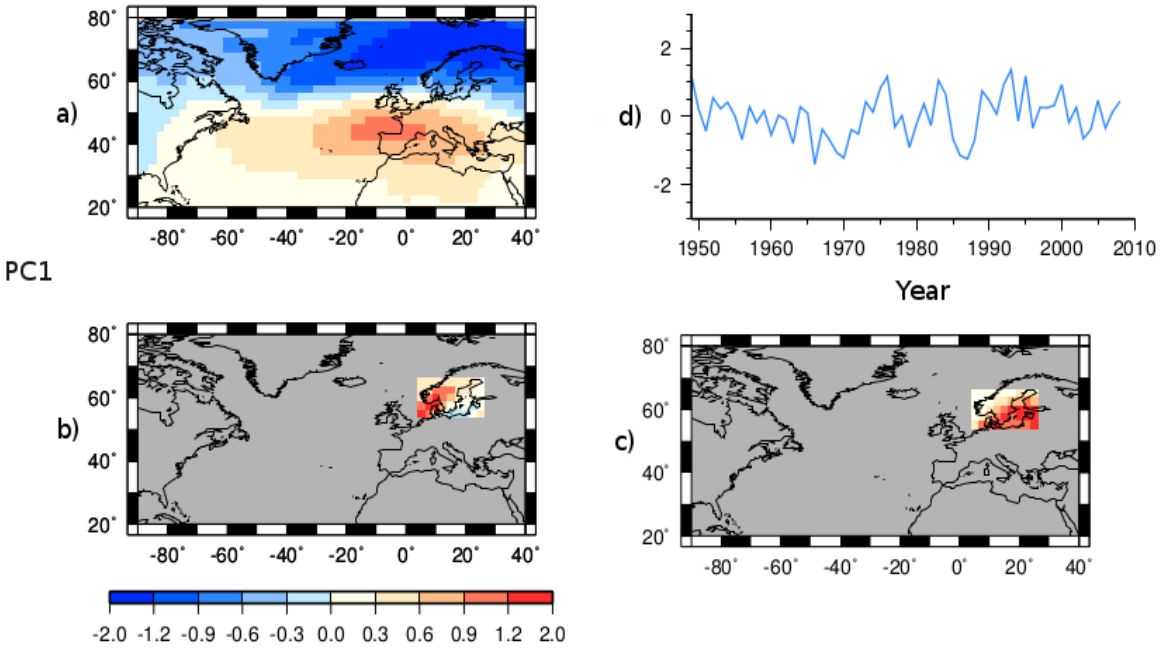

Figure 4.3: PC scores (d) and eigenvector loadings (a, b, c) describing the variation of winter sea level pressure (a), precipitation (b) and temperature (c) of the leading PC of PCAstp2. The grey temperature and precipitation fields were not included in PCAstp2.

Figure 4.3 shows the two leading PC of the PCAstp2 using NCEP/NCAR winter (DJF) sea level pressure, precipitation and temperature anomalies from 1949-2008. The sea level pressure variation pattern associated with the leading PC displays resemblance to the NAO winter pattern as described by NOAA-CPC (2012) and BARNSTON and LIVEZEY (1987), while the PC scores times series shows less resemblance with the NOAA-CPC (2012) NAO time series than the PC scores from PCAna and PCAnh. Associated with the sea level pressure variation pattern (Fig. 4.3a) are high

precipitation rates in southern Norway (Fig. 4.3b) and high temperatures in southern Sweden and over the Baltic Sea (Fig. 4.3c). The mode of variation described by the second PC of the PCAstp2(s) using summer (JJA) sea level pressure, precipitation and temperature anomalies from 1949-2008 displays a covariation of high sea level pressure over the central North Atlantic ocean and South-East Scandinavia with low sea level pressure over Greenland (Fig. 4.4a) and high temperatures over southern Scandinavia and the Baltic Sea (Fig. 4.4c). A negative trend in temporal evolution of the PC scores since the early 1990's is associated with this PC. The pattern of the negative centres of variation and their strong association with temperature is consistent with the nature of the summer Scandinavia pattern NOAA-CPC (2012).

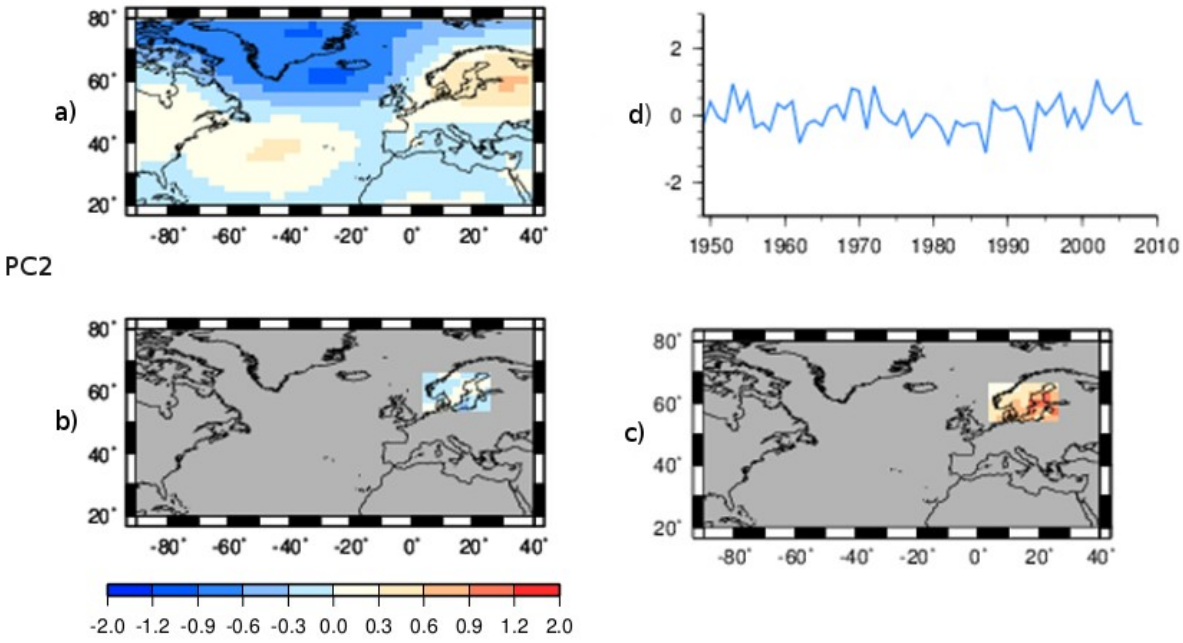

Figure 4.4: PC scores (d) and eigenvector loadings (a, b, c) describing the variation of summer sea level pressure (a), precipitation (b) and temperature (c) of the second PC of PCAstp2. The grey temperature and precipitation fields were not included in PCAstp2.

4.2 Correlation Between Glacier Mass Changes and Atmospheric Variables

This section describes the statistical dependence between glacial mass balance and the constructed atmospheric variables (section 3.2) as determined by correlation analyses described in section 3.3. While the atmospheric variables that serve as predictors to train the multiple regression model are constructed from NCEP/NCAR re-analysis data for reasons stated in section 2.2, the spatiotemporal means and stationary NAO indices constructed from ERA40 re-analysis data were used for analogous analyses to provide a comparison between correlation coefficients obtained from glacial mass balance and variables based on ERA40 re-analysis data and correlation coefficients obtained from glacial mass balance and variables based on NCEP/NCAR re-analysis data.

In disregard of the database, the highest correlation coefficients were obtained from six month seasonal air temperature and precipitation rate means, the stationary NAO indices, and a selection of principal component scores from PCA$_{NA}$, PCA$_{NH}$, PCA$_{STP1}$ and PCA$_{STP2}$. Unless stated otherwise, the focus of the descriptions lies on the glaciers and atmospheric variables used in the regression model. The significance of the Pearson correlation coefficients is expressed in terms of a 0.1, 0.005 or 0.1 value behind the coefficient value for *p*-value intervals 0.1-0.05, 0.05-0.01 and < 0.01 respectively. The correlation coefficients associated with a *p*-value of less than 0.1 are considered insignificant. For readability, the Pearson correlation coefficients will also be referred to as *r* values in this section. In this and the remaining chapters, he notation (w) and (s) following the PCA type indicates whether winter (DJF) or summer (JJA) means of sea level pressure were used in the mentioned PCA. The word dependence is used to refer to the linear stochastic dependence as determined by the correlation analyses (section 3.3). Since the length of the glacial mass balance time series varies and therefore the sample size for the correlation analyses also varies, this sections refers to the common temporal coverage of the analysed variables as their temporal overlap.

4.2.1 Precipitation Rate – Mass Balance Correlation

This sub-section describes the magnitude and identified patterns in Pearson correlation coefficients calculated from spatiotemporal means of precipitation rates and glacial mass balance. Descriptions focus on the correlation between the six month means and mass balance, as they showed as stronger stochastic dependence with the mass balance time series than the three month means. Thus, winter refers to the ONDJFM season, and summer refers to the AMJJAS season.

The Pearson correlation coefficients calculated from the total temporal overlaps of the NCEP/NCAR precipitation rate winter means and glacial winter mass balance time series range from 0.71(0.01) for Ålfotbreen to 0.44(0.1) for Gråsubreen and 0.34 (0.05) for Engabreen. Figure 4.6 (second from bottom) shows the normalised anomalies of glacier winter mass balance (colour coded) and the spatiotemporal means of winter precipitation rates to provide the reader with a visual idea of their correlation. For the temporal overlaps within the 1949-1988 time span, slightly lower r values are obtained for most glaciers. These range from 0.71(0.01) for Ålfotbreen, 0.41(0.1) for Gråsubreen, and no significant r for Engabreen. For the temporal overlaps within the 1989-2008 time span, the highest correlation coefficients are obtained, ranging from 0.91(0.01) for Ålfotbreen to 0.57(0.05) for Gråsubreen. The Pearson correlation coefficients calculated from the total temporal overlaps of the NCEP/NCAR precipitation rate summer means and glacial summer mass balance range are predominantly negative or insignificant.

The correlation analyses using ERA40 re-analysis data as a basis for precipitation rate means yield similar results. The r values calculated from winter precipitation and mass balance range from 0.69(0.01) for Ålfotbreen to 0.37(0.01) for Gråsubreen, from 0.67(0.01) for Ålfotbreen to 0.30(0.1) for Gråsubreen and from 0.83(0.01) for Ålfotbreen to 0.57(0.05) for Gråsubreen using the temporal overlaps within the 1949-2008, 1949-1988 and 1989-2008 respectively. The correlation analyses using the Engabreen mass balance time series yields no significant correlation coefficients for any investigated time span. The Pearson correlation coefficients calculated from the total temporal overlaps of the ERA40

precipitation rate summer means and glacial summer mass balance are predominantly negative or insignificant.

In disregard of the database used for the construction of the atmospheric variables, the decrease in *r* values calculated from winter precipitation and winter mass balance roughly corresponds to the distance of the glacier from the coast for the glaciers lying on approximately the same latitude.

4.2.2 Surface Temperature – Mass Balance Correlation

This sub-section describes the magnitude and identified patterns in Pearson correlation coefficients calculated from spatiotemporal means of surface temperatures and glacial mass balance. Descriptions focus on the correlation between the six month means and mass balance, as they showed as stronger stochastic dependence with the mass balance time series than the three month means. As in the previous sub-section, winter refers to the ONDJFM season, and summer refers to the AMJJAS season.

The Pearson correlation coefficients calculated from the total temporal overlaps of the NCEP/NCAR surface temperature winter means and glacial winter mass balance time series range from 0.64(0.01) for Ålfotbreen to 0.30(0.05) for Gråsubreen. Figure 4.6 (bottom) shows the normalised anomalies of glacier winter mass balance (colour coded) and the spatiotemporal means of winter temperature to provide the reader with a visual idea of their correlation. For the temporal overlaps within the 1949-1988 time period, slightly lower *r* values are obtained for most glaciers, while the end members of the range remain the same. Using the Ålfotbreen winter mass balance yields an *r* value of 0.59(0.01), while using the data from Gråsubreen yields an *r* value of 0.27(0.1). For the temporal overlaps within the 1989-2008 time period, a slightly higher *r* values were obtained for most glaciers. These range from 0.81(0.01) for Ålfotbreen and 0.66(0.01) for Engabreen, while no significant correlation between winter temperature and Gråsubreen were obtained.

The correlation analyses using NCEP/NCAR surface temperature summer means and summer mass balance time series yield only negative correlation coefficients. For the total temporal overlaps of these, *r* values range from -0.70(0.01) for Ålfotbreen to -0.40(0.01) for Engabreen. For the

temporal overlaps within the 1949-1988 time period, the *r* values range from -0.64(0.01) for Storbreen and -0.35(0.1) for Engabreen. The correlation coefficients calculated from temporal overlaps in the 1989-2008 time period have a smaller range from -0.61(0.01) for Gråsubreen to -0.53(0.05) for Storbreen. Figure 4.5 (bottom) shows the normalised anomalies of glacier summer mass balance (colour coded) and the spatiotemporal means of summer temperature to provide the reader with a visual idea of their correlation.

The magnitude of difference between correlation coefficients calculated from analyses using NCEP/NCAR data and those calculated from analyses using the ERA40 data is comparable to the magnitude of difference seen in the previous section. The correlation coefficients calculated using ERA40 data are slightly lower, while the distribution of *r* values among the glaciers remains similar.

4.2.3 Stationary NAOi – Mass Balance Correlation

This sub-section describes the magnitude and identified patterns in Pearson correlation coefficients calculated from the stationary NAO indices (section 3.2.2) and glacial mass balance.

The correlation analyses using the NCEP/NCAR derived indices for the winter and summer NAO and glacial winter mass balance time series within the temporal overlaps of the datasets mostly yield no significant or low *r* values within a 0.3 ± 0.1 range. Likewise, carrying out the analysis for the summer season yields no significant or low negative *r* values with a similar range of magnitude.

The Pearson correlation coefficients calculated from the total temporal overlaps of the ERA40 derived Gibraltar-Reykjavik winter NAO index and glacial winter mass balance time series range from 0.56(0.01) for Nigardsbreen to 0.30(0.05) for Engabreen. The Lissabon-Reykjavik and Ponta Delgarda-Reykjavik indices score slightly higher *r* values, ranging from 0.61(0.01) for Nigardsbreen to 0.33(0.05) for Engabreen, and from 0.62(0.01) for Nigardsbreen to 0.34(0.05) for Engabreen respectively.

The analyses for the summer season yield negative *r* values in the range of -0.3 ± 0.1. The highest *r* values of ca. -0.4(0.01) are achieved in the

analyses using Storbreen summer mass balance, while Nigardsbreen mass balance shows no significant dependence with any of the stationary summer NAO indices.

4.2.4 Sea Level Pressure Principal Components – Mass Balance Correlation

This sub-section describes the magnitude and identified patterns in Pearson correlation coefficients calculated from the principal components of PCA$_{NA}$, PCA$_{NH}$, PCA$_{STP1}$ and PCA$_{STP2}$ and glacial mass balance. The descriptions focus on the principal components and seasons marked by strong stochastic relationships between a PC and glacial mass balance. The PCAs used the sea level pressure of the NCEP/NCAR re-analyses as a database. In this sub-section, winter and summer in context of PCAs refers to DJF and JJA season respectively. PC scores from spring (MAM) and autumn (SON) seasons produce few, low or no significant *r* values.

The Pearson correlation coefficients calculated from the total temporal overlaps of glacial winter mass balance time series and the PC scores of the first PC of PCA$_{NA}$(w) range from 0.82(0.01) for Ålfotbreen to 0.30(0.05) for Gråsubreen. Figure 4.6 (top) shows the normalised anomalies of glacier winter mass balance (colour coded) and the PC scores of the first PC of PCA$_{NA}$(w) to provide the reader with a visual idea of their correlation. For the temporal overlaps within the 1949-1988 time period, slightly lower *r* values are obtained for most glaciers. They range from 0.74(0.01) for Ålfotbreen to 0.39(0.05) for Hellstugubreen. No significant correlation was found for Gråsubreen. The highest *r* values are obtained for the temporal overlaps within the 1989-2008 time period, ranging from 0.88(0.01) for Ålfotbreen to 0.36(0.05) for Gråsubreen. No significant correlation was found for Engabreen. In all of the investigated time period, the decrease in *r* values roughly corresponds to the distance of the glacier from the coast. The *r* values for Engabreen, the most northern glacier, are also among the lowest. The analyses using PC scores of the first PC of PCA$_{NA}$(s) and glacial summer mass balance only yielded significant *r* values for Ålfotbreen (0.36) and Engabreen (0.31) in the temporal overlap within the 1949-1988 time period.

The Pearson correlation coefficients calculated from the total temporal overlaps of glacial winter mass balance time series and the PC scores of the second PC of PCANA(w) range from -0.42(0.01) for Gråsubreen to -0.32(0.01) for Hardangerjøkelen. For the temporal overlaps within the 1949-1988 and 1989-2008 time periods, *r* values range from -0.38(0.05) for Hellstugubreen to -0.26(0.1) for Ålfotbreen and from -0.73(0.01) for Gråsubreen to -0.42(0.01) for Ålfotbreen respectively. The analyses using PC scores of the second PC of PCANA(s) and glacial summer mass balance yields *r* values in a -0.3 ± 0.1 interval for the total temporal overlaps, *r* values in a -0.45 ± 0.1 interval for the temporal overlaps within the 1949-1988 time period, and *r* values in a -0.35 ± 0.1 interval for the temporal overlaps within the 1989-2008 time period.

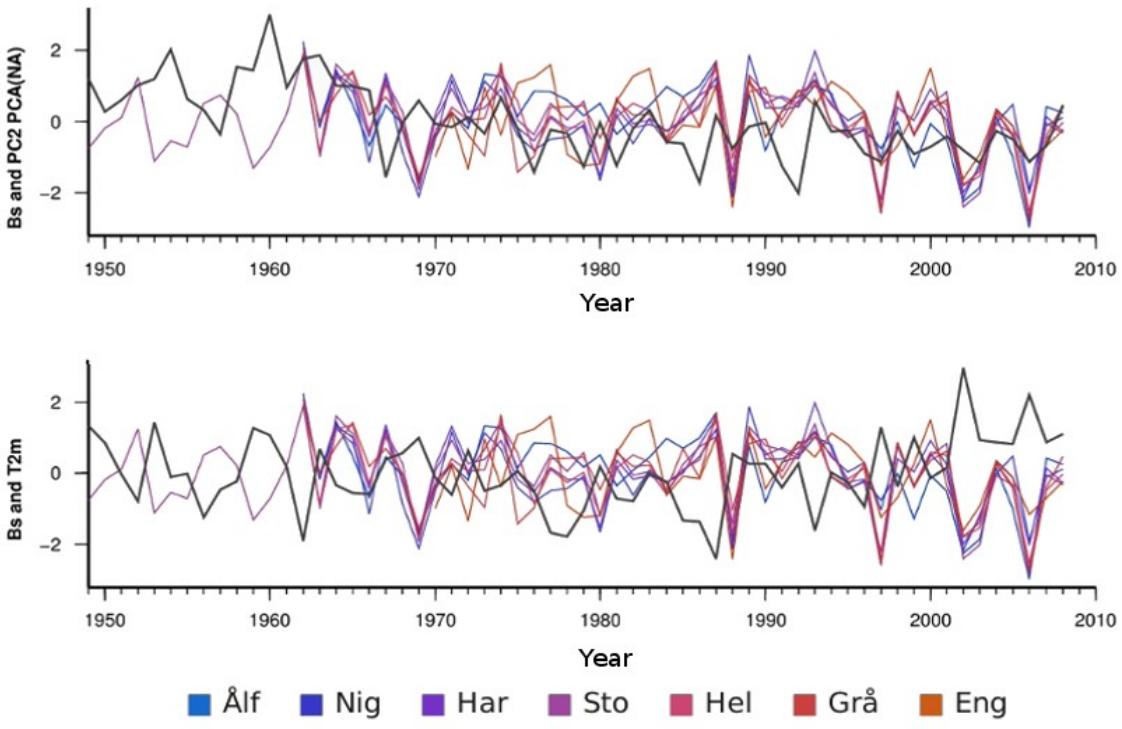

Figure 4.5: Normalised anomalies of summer mass balance (colour coded), the PC scores of the second PC of PCANA(s) (top) and summer air temperature (bottom).

In winter and summer, no apparent East-West gradient of *r* value can be recognised. Figure 4.5 (top) shows the normalised anomalies of glacier

summer mass balance (colour coded) and the PC scores of the second PC of PCA$_{NA}$(s) to provide the reader with a visual idea of their correlation.

The Pearson correlation coefficients calculated from the total temporal overlaps of glacial winter mass balance time series and the PC scores of the first PC of PCA$_{NH}$(w) range from 0.70(0.01) for Ålfotbreen to 0.27(0.05) for Gråsubreen. Figure 4.6 (top) shows the normalised anomalies of glacier winter mass balance (colour coded) and the PC scores of the first PC of PCA$_{NH}$(w) to provide the reader with a visual idea of their correlation. For the temporal overlaps within the 1949-1988 time period, *r* values range from 0.70(0.01) for Ålfotbreen to 0.39(0.05) for Hellstugubreen, while no significant correlation between the PC scores and the Gråsubreen mass balance can be found. The correlation coefficients obtained from temporal overlaps within the 1989-2008 time period are within a 0.5 ± 0.1 interval. No significant *r* values are found for the Gråsubreen, Hellstugubreen and Storbreen winter mass balance time series. The correlation analyses using glacial summer mass balance and the PC scores of the first PC of PCA$_{NH}$(s) only yield significant correlation coefficients for the temporal overlaps within the 1949-1988 time period. Those are within a 0.3 ± 0.05 interval. In winter, the strength of the relationship decreases with the distance of the glacier from the coast. In summer, no apparent East-West gradient for *r* values can be recognised.

The Pearson correlation coefficients calculated from the total temporal overlaps of glacial summer mass balance time series and the PC scores of the fourth PC of PCA$_{NH}$(s) are in a -0.35 ± 0.1 interval. For the overlaps within the 1989-2008 time span, the *r* values are in a -0.5 ± 0.1 interval, while no significant *r* values were calculated for the overlaps within the 1949-1988 time span.

The PC scores of the first PC of PCA$_{STP2}$(w) achieve similar results as the PC scores of the first PC of PCA$_{NA}$(w) in the analyses with glacial winter mass balance time series, but the *r* values are slightly lower for most glaciers and time spans. The highest correlation coefficients were calculated for the temporal overlaps within the 1989-2008 time span, followed by the correlation coefficients calculated for the total temporal

overlaps. The strength of the relationship decreases for Engabreen and glaciers that are located farther away from the coast.

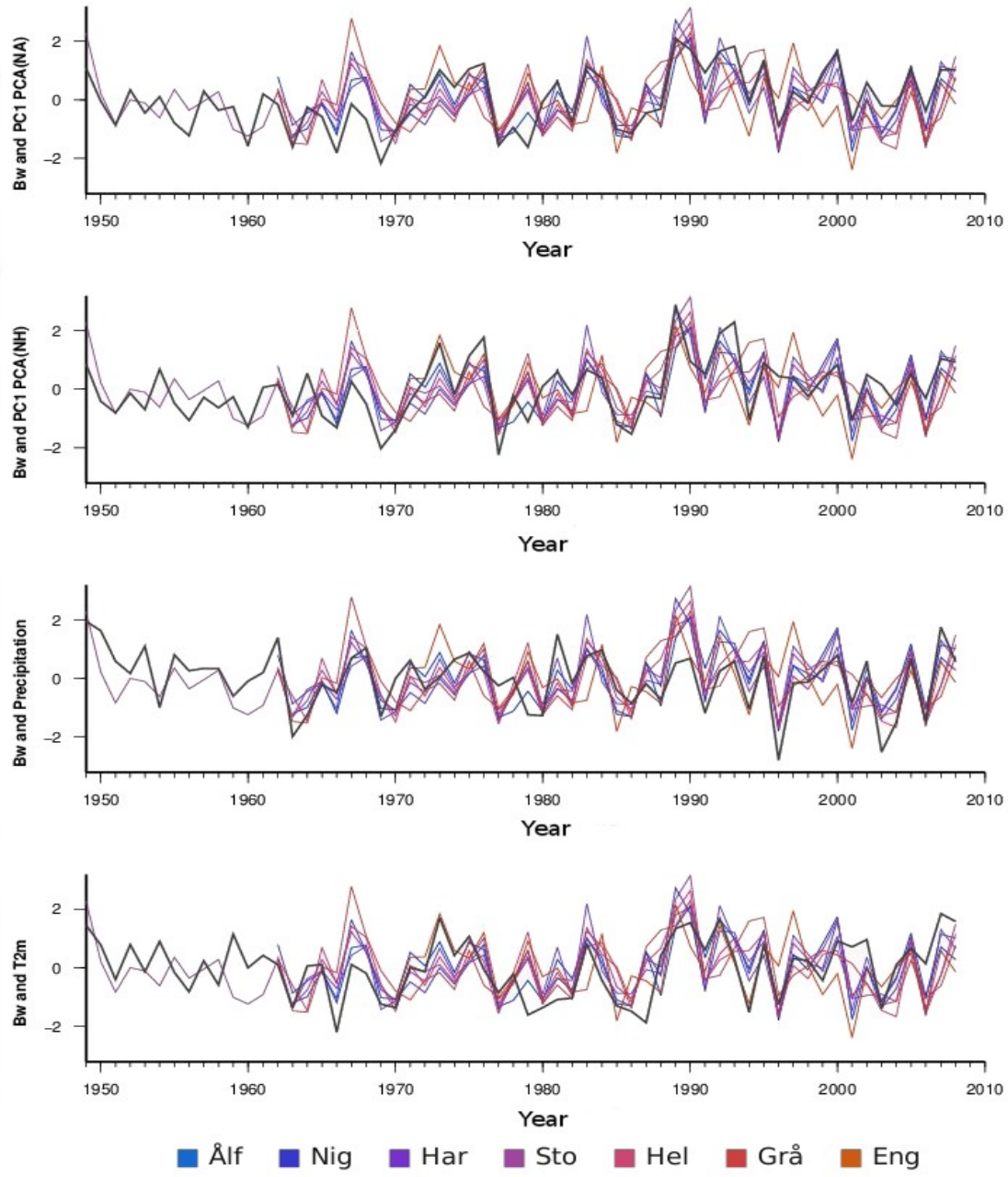

Figure 4.6: Normalised anomalies of winter mass balance (colour coded), the PC scores of the first PC of PCA$_{NA}$(w) (top), the PC scores of the first PC of PCA$_{NH}$(w) (second from top), winter precipitation (second from bottom) and winter air temperature (bottom).

The PC scores of the second PC of PCA$_{STP2}$(s) achieve similar results as the PC scores of the second PC of PCA$_{NA}$(s) in the analyses with glacial winter mass balance time series, but the *r* values are slightly higher for the total temporal overlap of the time series.
The PC scores of the first PC of PCA$_{STP1}$(w) achieve similar results as the PC scores of the first PCs of PCA$_{NA}$(w) and PCA$_{STP2}$(w) in the analyses with glacial winter mass balance time series, but the *r* values are lower for most glaciers and time spans.

4.2.5 Correlation Coefficients from Moving Time Windows

This sub-section describes the results of the correlation analyses using moving 10 year time windows to track changes in *r* values over time (section 3.3). The most radical changes in correlation coefficients over time show for the correlation between glacial winter mass balance and the PC scores of the first PC of PCA$_{NA}$ using winter (DJF) sea level pressure (Fig. 4.7). In figure 4.7, the *r* values are assigned to the middle year of the 10 year time window they are calculated from. It shows a notable shift in *r* values from the 1980-1989 to the 1981-1990 time window. The correlation coefficients for glaciers in coastal proximity, represented by blue colours, are higher than those for the glaciers further away from the coast, represented by red colours. The correlation coefficients for the more northern Engabreen are represented by the colour orange. The correlation coefficients for calculated from 10 year time windows of winter (ONDJFM) temperature means and glacial winter mass balance show a similar, but less pronounced shift at the same time.

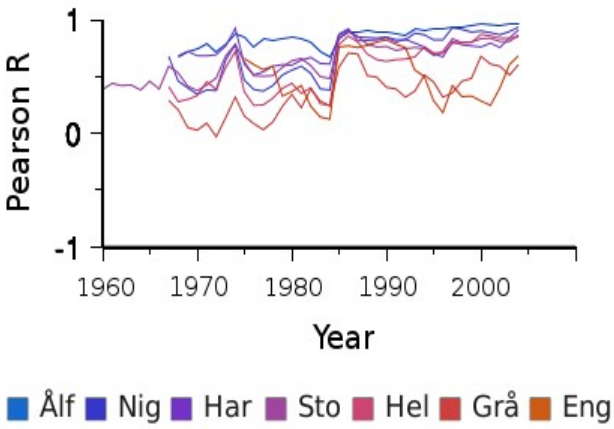

Figure 4.7: Pearson correlation coefficients from correlation analyses using the winter mass balance of different glaciers (colour coded) and the PC scores of the first PC of PCA$_{NA}$(w) using moving 10 year time windows.

The correlation coefficients calculated from moving 10 year windows of glacial summer mass balance and spatiotemporal means of air temperature in the six months ablation season (AMJJAS) shift from negative values in the 1970's to positive values in the 1980's and 1990's and return to slightly negative values in the 2000's.

4.3 Impact of Mid-Latitude Atmospheric Variability on Glacial Mass Balance

This section describes the results of the multiple regression analyses described in section 3.3. The analyses were carried out with three different sets of predictors. The first predictor set includes PC scores from PC1-PC5 of PCA$_{NA}$, temperature and precipitation rate means, the second is comprised of PC scores from PC1-PC5 of PCA$_{NH}$, temperature and precipitation rate means, and the third uses the PC scores of the 12 leading PCs of PCA$_{STP2}$. The notation (w) and (s) following the PCA type indicates whether winter (DJF) or summer (JJA) means of sea level pressure were used in the mentioned PCA. In this section, the term explained variance is used as described in section 3.2.3. The glaciers in figure 4.8, figure 4.9 and figure 4.10 are sorted by their distance from the coast. The leftmost is the glacier that is closest to the coast. The northern glacier Engabreen is placed to the right of the glacier with the greatest distance from the coast.
In the multiple regression analyses using the first predictor set, most of the winter mass balance variances in time periods 1949-2008 and 1989-2008 are explained by the PC scores of the first PC of PCA$_{NA}$(w) (Fig. 4.8 top), while temperature and PC scores of the third and fourth PC of PCA$_{NA}$(w) are dominant in the 1949-1988 time period. The amount of explained variance ranges from 90% - 47% in the 1989-2008 time period, from 77% - 30% in the 1949-2008 time period and from 50% - 19% in the 1949-1988 time period. In time periods 1949-2008 and 1949-1988, the amount of explained variance decreases with the increase in distance of the glacier to the coast. The least amount of variance in all time periods is explained for the Engabreen winter mass balance.

Most of the explained summer mass balance variances are explained by temperature and the PC scores of the second, third and fifth PC of PCANA(s) (Fig 4.8 bottom). In the 1949-2008 time period, the dominant predictors are the third and fifth PC of PCANA(s). In the 1989-2008 time period, the dominant predictor is the second PC of PCANA(s). The amount of explained variance ranges from 69% - 21% in the 1989-2008 time period, from 59% - 31% in the 1949-2008 time period and from 53% - 19% in the 1949-1988 time period. As for the winter season, the explained predictand variances are highest in the 1989-2008 time period, followed by the explained variances in the 1949-2008 time period.

Overall, the predictors of the first predictor set explain more of the glacial winter mass balance than of the glacial summer mass balance in time periods 1949-2008 and 1989-2008. In the 1949-1988 time period, the least amount of of predictand variance is explained in winter and summer.

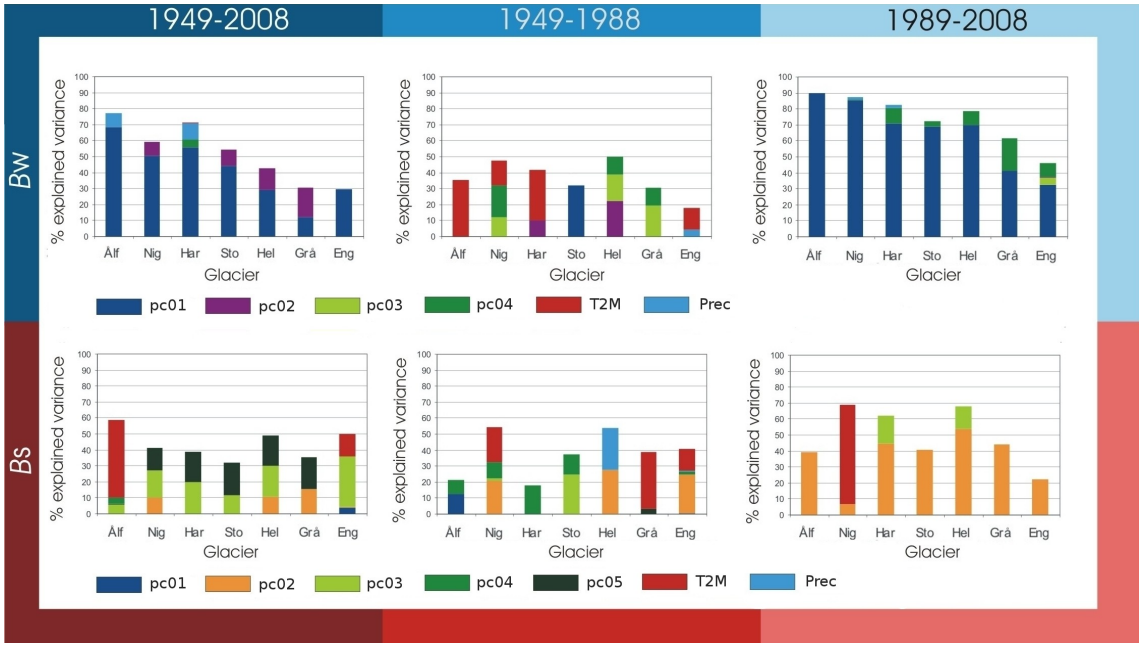

Figure 4.8: Amount of mass balance variance explained by predictors (colour coded) from the first predictor set in winter (top) and summer (bottom) for time periods 1949-2008 (left), 1949-1988 (centre) and 1989-2008 (right). Predictors include PC scores (pc01-pc05), temperature (T2M) and precipitation (Prec)

The multiple regression analyses computed with the second predictor set yield similar results for the winter season. Most of the winter mass balance variances in time periods 1949-2008 and 1989-2008 is explained by the PC scores of the first and second PC of PCA$_{NH}$(w) (Fig. 4.9 top), while temperature and PC scores of the third and fifth PC of PCA$_{NH}$(w) are dominant in the 1949-1988 time period. The amount of explained variance ranges from 90% - 46% in the 1989-2008 time period, from 78% - 21% in the 1949-2008 time period and from 53% - 30% in the 1949-1988 time period. In time periods 1949-2008 and 1949-1988, the amount of explained variance decreases with the increase in distance of the glacier to the coast. The amount of variance explained for the Engabreen winter mass balance is higher than that in the multiple regression analyses using the first predictor set. Temperature contributes most to the explained summer mass balance variances (Fig. 4.9 bottom). The amount of explained variance ranges from 69% - 19% in the 1989-2008 time period, from 47% - 1% in the 1949-2008 time period and from 40% - 5% in the 1949-1988 time period. The explained predictand variances are highest in the 1989-2008 time period. The explained predictand variances in the 1949-2008 and 1949-1988 time periods are significantly lower on average.

Overall, the predictors of the second predictor set explain more of the glacial winter mass balance than of the glacial summer mass balance in all time periods.

In the multiple regression analyses using the third predictor set, the PC scores of the first PC of PCA$_{STP2}$(w) contribute most to the explained winter mass balance variances in all time periods (Fig. 4.10 top). The amount of explained variance ranges from 69% - 28% in the 1989-2008 time period, from 54% - 32% in the 1949-2008 time period and from 53% - 0% in the 1949-1988 time period.

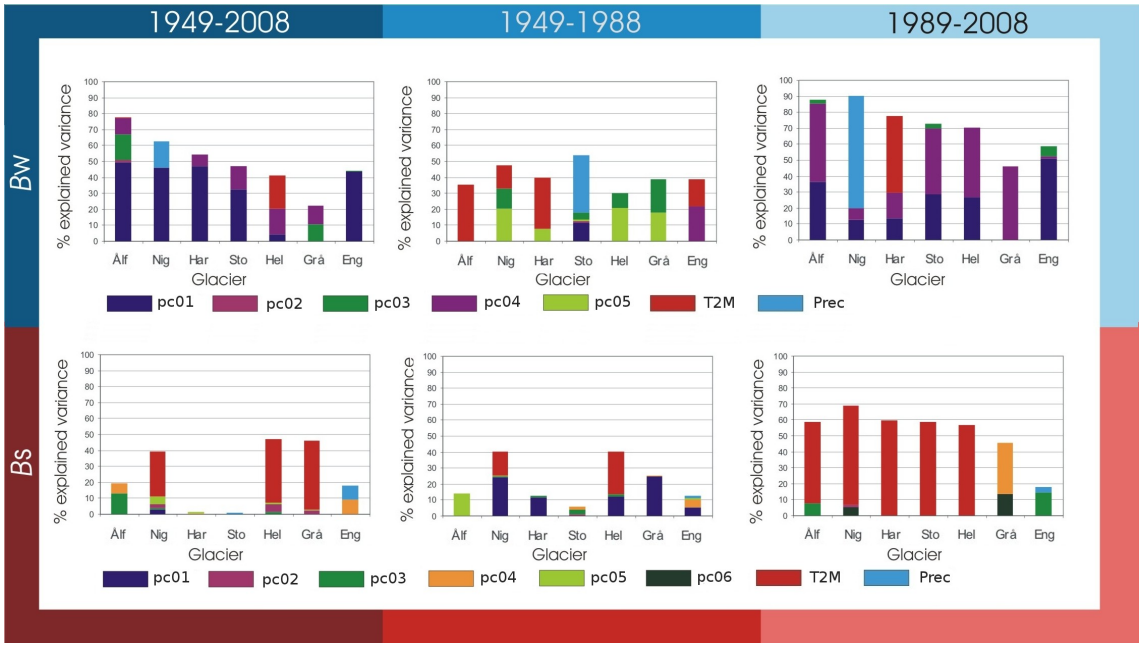

Figure 4.9: Amount of mass balance variance explained by predictors (colour coded) from the second predictor set in winter (top) and summer (bottom) for time periods 1949-2008 (left), 1949-1988 (centre) and 1989-2008 (right). Predictors include PC scores (pc01-pc06), temperature (T2M) and precipitation (Prec).

The PC scores of the second PC of PCAstp2(s) contributes most to the explained summer mass balance variances (Fig. 4.10 bottom). The amount of explained variance ranges from 87% - 50% in the 1989-2008 time period, from 54% - 28% in the 1949-2008 time period and from 22% - 0% in the 1949-1988 time period. The explained predictand variances are highest in the 1989-2008 time period, followed by the explained variances in the 1949-2008 time period. The explained predictand variances 1949-1988 time period are significantly lower on average.

On average, the predictors of the third predictor set explain more of the glacial summer mass balance than of the glacial winter mass balance in time periods 1949-2008 and 1989-2008. The predictors of the third predictor set explain more of the glacial summer mass balance in 1989-2008 than the first and second predictor sets. The amount of explained variance averaged over all glaciers, seasons and time periods is highest for the first predictor set.

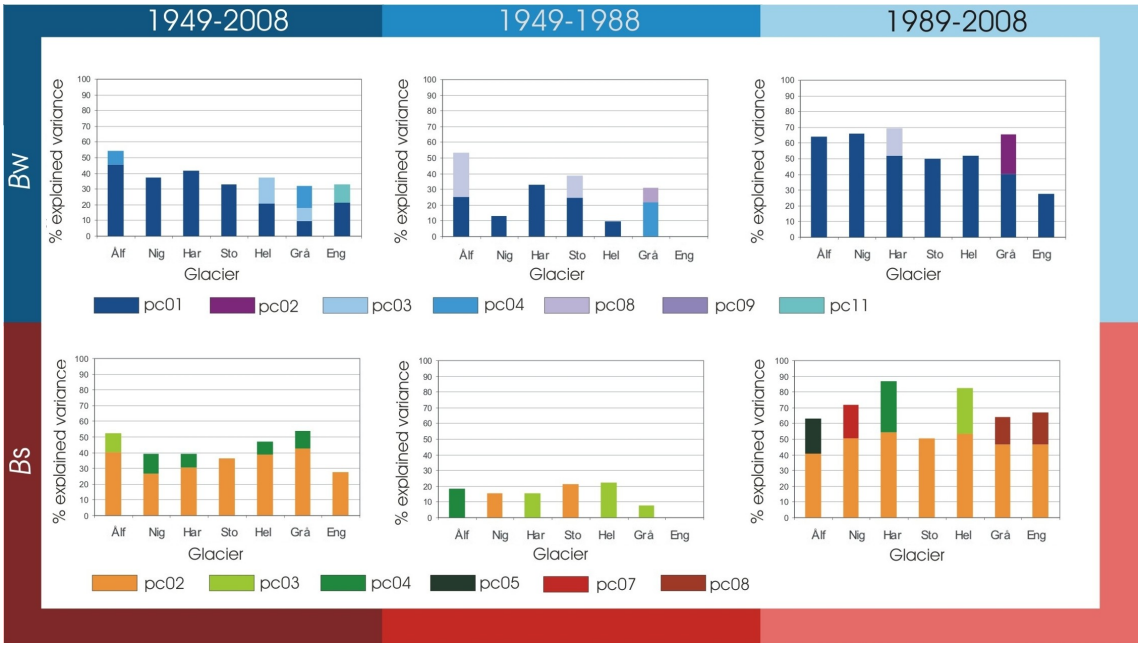

Figure 4.10: Amount of mass balance variance explained by predictors (colour coded) from the third predictor set in winter (top) and summer (bottom) for time periods 1949-2008 (left), 1949-1988 (centre) and 1989-2008 (right). Predictors include PC scores of the leading 12 PCs (pc01-pc12).

5 Glacier Mass Balance Estimates

In the previous chapter, the results of multiple regression analyses with several sets of predictors were presented. On average, the set of predictors including the PC scores of PCA$_{NA}$, and six moth seasonal surface temperature and precipitation rate means performed best at explaining the variance of glacial mass balance. Consequently, following the procedures described in section 3.4, the multiple regression models trained with this predictor set were used for the generation of the glacial mass balance estimates with the aid of the predictors reconstructed from the CMIP3 model dataset. The estimates were made for each model, climate scenario, model run, season, glacier, and training time periods (1949-2008, 1949-1988 and 1989-2008) separately. The 18 chosen models (section 2.2), climate scenarios, individual model runs per scenario, two seasons, seven glaciers and three different time periods generate a total of 5,922 individual time series estimates, 2,520 ensemble mean estimates when averaged over the individual runs, and 168 multi-model mean estimates when averaging the ensemble mean estimates over the different models. Many estimates of future winter mass balance generated from individual simulations show a significant positive trend from 2000 to 2100 for model simulations that predict a positive trend for NAO index values. These trends are strongest for the most maritime glaciers. According to most estimates, summer melting also increases over the 2000-2100 time period. Given the large number of individual estimates, the presentation of results is reduced to examples of ensemble means of estimates and a multi-model ensemble mean summary of cumulative net mass balance estimates.

5.1 ECHAM5 Ensemble Means of Estimates

This section outlines examples of ensemble means of estimates. The two glaciers, for which mass balance estimates are described here, represent the two end members of the maritime-continentality range in this study. The choice of the climate model is arbitrary. The estimates presented here were made from the predictors constructed from ECHAM5 simulations and the multiple regression model trained in the 1949-2008 time period.

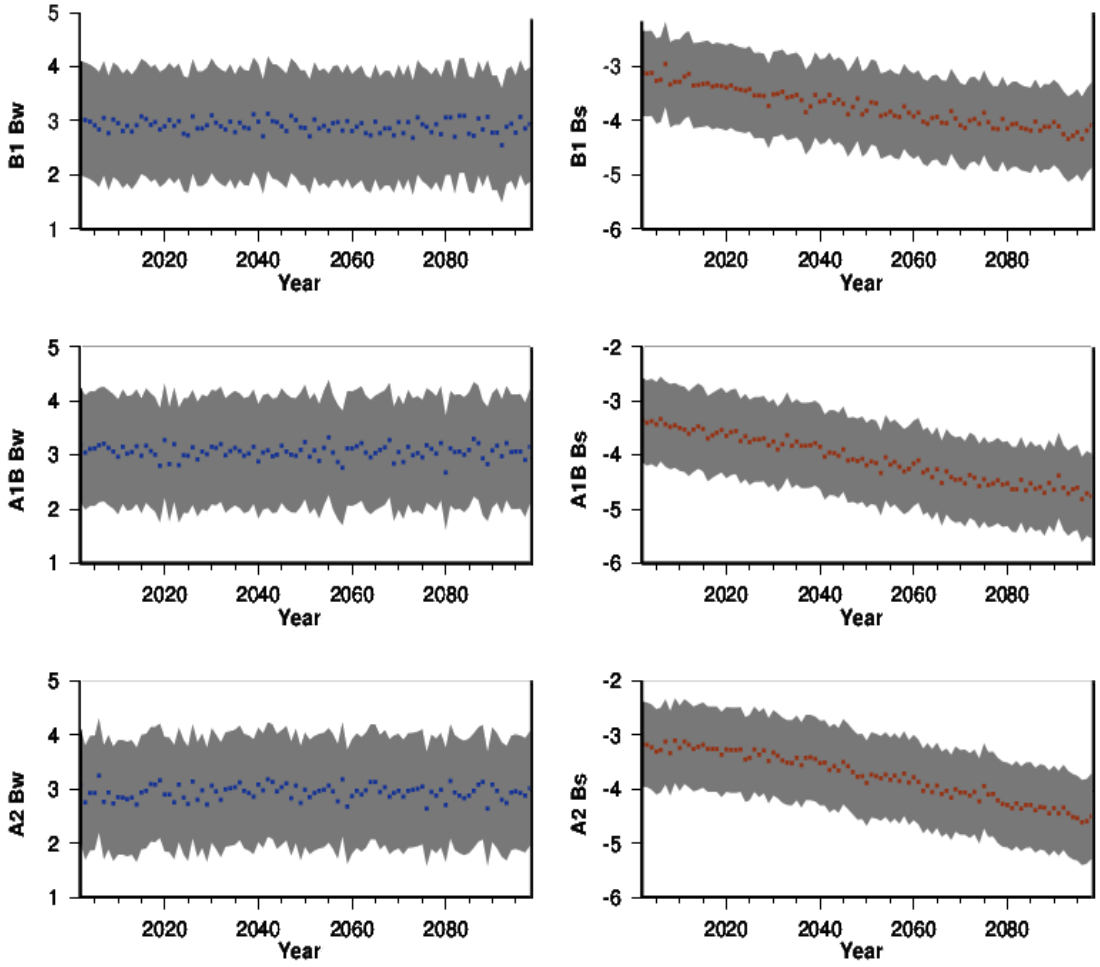

Figure 5.1: ECHAM5 ensemble means of Ålfotbreen winter (left) and summer (right) mass balance estimates for the time period 2000-2100 and scenarios B1 (top), A1B (centre) and A2 (bottom) from the regression model trained in the 1949-2008 time period.

Figure 5.1 shows the ensemble means of winter and summer mass balance point and interval estimates (section 3.4) for Ålfotbreen for the three future

climate scenarios. While there is no significant trend of winter mass balance values from present day to the year 2100 for any future scenario, summer glacial mass loss increases with time. In the A1B and A2 scenarios, the summer glacial mass loss shows a greater increase than in the B1 scenario.

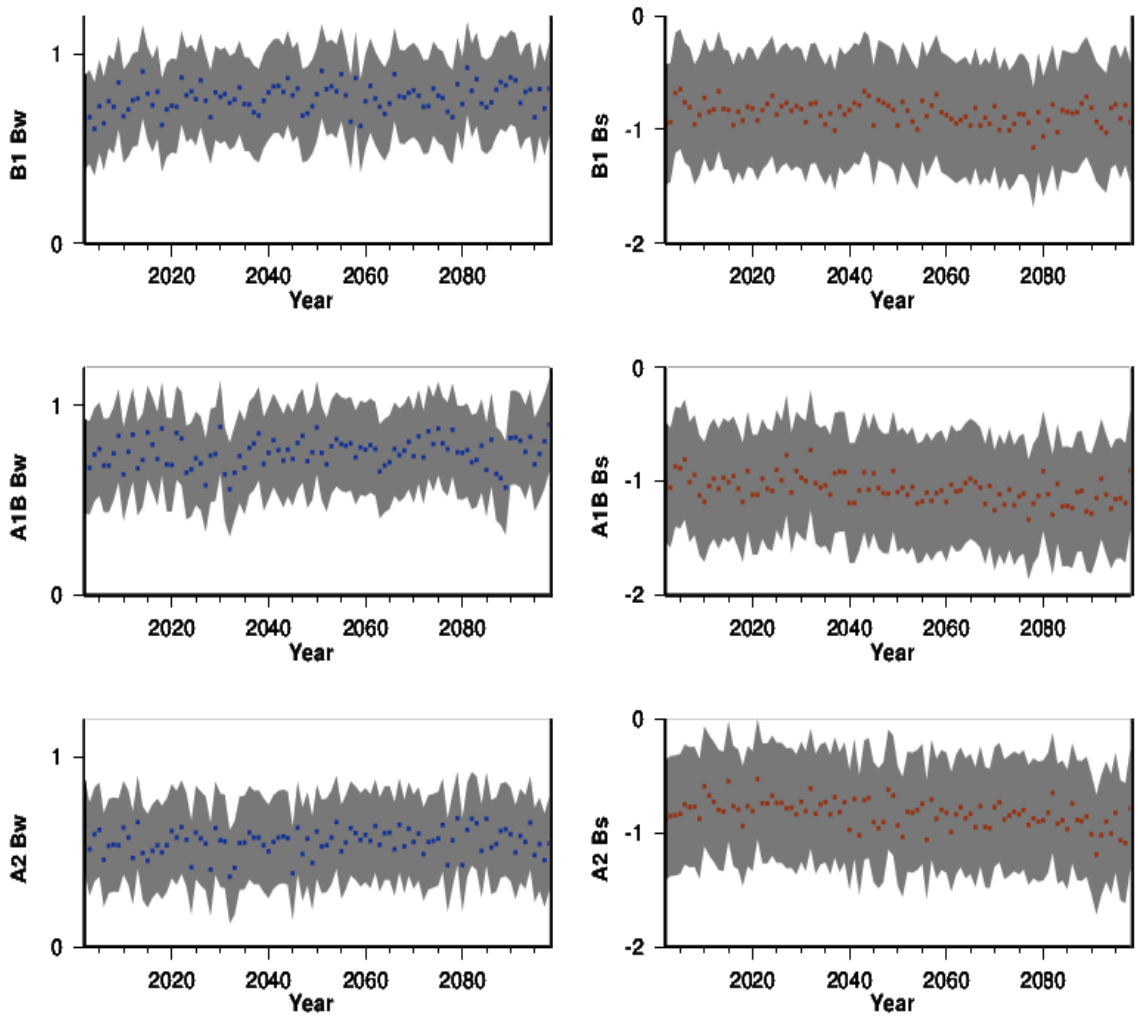

Figure 5.2: ECHAM5 ensemble means of Gråsubreen winter (left) and summer (right) mass balance estimates for the time period 2000-2100 and scenarios B1 (top), A1B (centre) and A2 (bottom) from the regression model trained in the 1949-2008 time period.

Figure 5.2 shows the ensemble means of winter and summer mass balance point and interval estimates (section 3.4) for Gråsubreen for the three future climate scenarios. While there is no significant trend of winter mass

balance values from present day to the year 2100 for any future scenario, summer glacial mass loss increases slightly in the A1B and A2 scenarios.
In disregard of the scenario, the predicted winter mass gain of Ålfotbreen is always greater than that of Gråsubreen. Likewise, the predicted summer mass loss is also greater for Ålfotbreen than for Gråsubreen. Independent of the training time period for the regression models, similar negative summer mass balance trends show for most models. However, the temporal evolution of winter mass balance mostly varies from a weak negative to a positive trend depending on the model and scenario. The estimated summer and winter mass balance values are generally higher for glaciers closer to the coast than for glaciers further inland.

5.2 Multi-Model Ensemble Means of Estimates

This section shows the multi-model mean glacial net mass balance estimates for the three future scenarios. The results for the regression models trained by the 1949-2008, 1949-1988 and 1989-2008 time periods are described separately.
Cumulative net mass balances calculated from multi-model ensembles of summer and winter mass balance estimates range from a ~50 m.w.e. mass surplus to a ~100 m.w.e. mass deficit by the year 2100. Figure 5.3 shows the multi-model cumulative net mass balance estimates for the time period 2000-2100. The estimates for glaciers in coastal proximity, represented by blue colours, are higher than those for the glaciers further away from the coast, represented by red colours. The estimates for Engabreen is represented by an orange hue. The different model training time periods are arranged in columns, while the different scenarios are arranged in rows.
The mass balance estimates generated from the model trained in the 1949-1988 time period digress most from each other. At the end of the 100 year time span, the cumulative net mass balance for Engabreen, Hardangerjøkelen and Ålfotbreen are positive, while the estimates for Hellstugubreen, Nigardsbreen, Gråsubreen and Storbreen are negative. The predicted net mass balance for Nigardsbreen remains approximately

zero for the first decades into the 21st century, but experiences a shift into negative net mass balance in the late decades of the century.

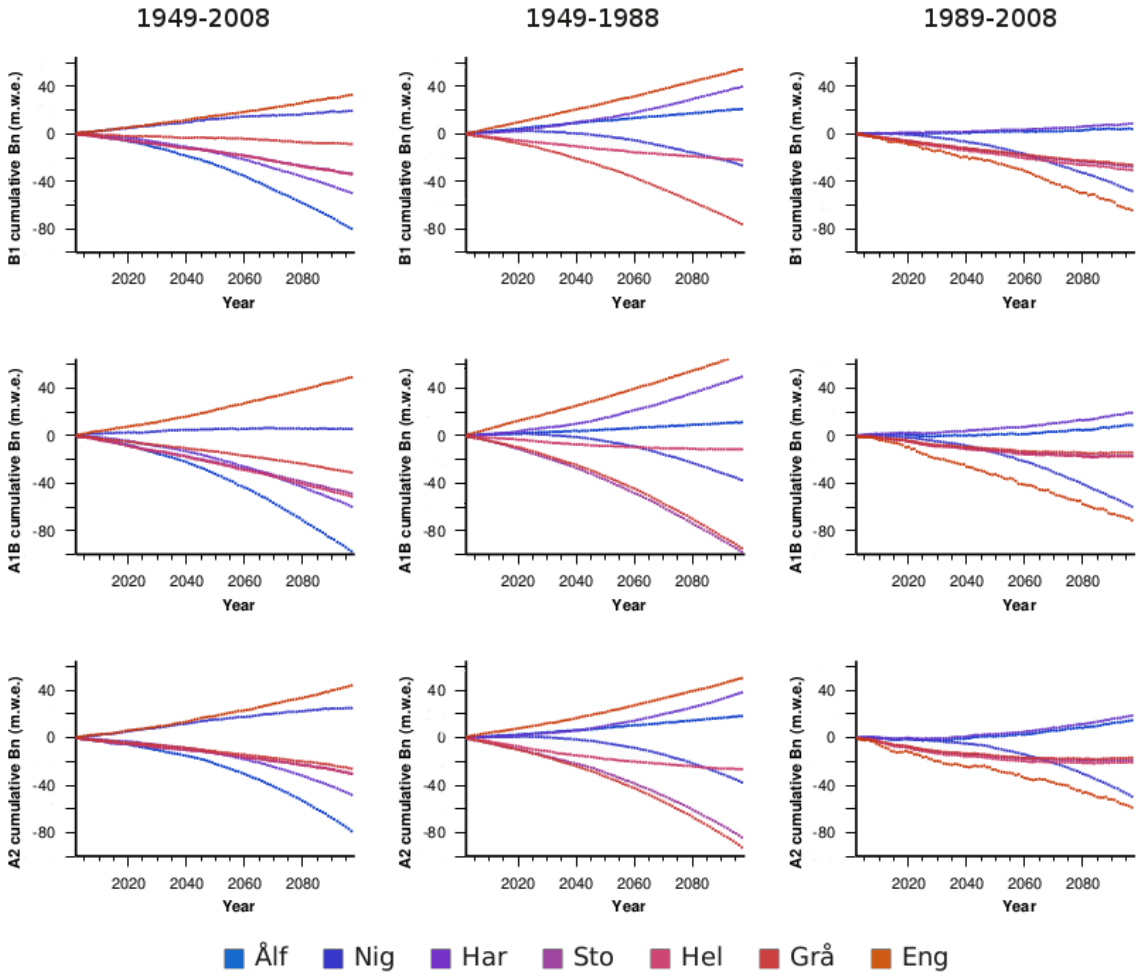

Figure 5.3: Multi-model ensemble means of net mass balance estimates for different glaciers (colour coded) for the time period 2000-2100, scenarios B1 (top), A1B (centre) and A2 (bottom) from regression models trained in the 1949-2008 (left), 1949-1988 (centre) and 1989-2008 (right) time periods.

The mass balance estimates generated from the model trained in the 1989-2008 time period are predominantly negative and digress least from each other. At the end of the 100 year time span, the cumulative net mass balance for Hardangerjøkelen and Ålfotbreen are positive, while the estimates for Gråsubreen, Storbreen, Hellstugubreen, Nigardsbreen and Engabreen are negative. Similar to the net mass balance estimates generated by the model trained in the 1949-1988 time period, the net mass

balance estimates for Nigardsbreen generated by the model trained in the 1989-2008 time period remains approximately zero for the first decades into the 21st century, but experiences a shift into negative net mass balance in the late decades of the century.

The mass balance estimates generated from the model trained in the 1949-2008 time period are predominantly negative. At the end of the 100 year time span, the cumulative net mass balance for Engabreen and Nigardsbreen are positive, while the estimates for Gråsubreen, Storbreen, Hellstugubreen, Hardangerjøkelen and Ålfotbreen are negative.

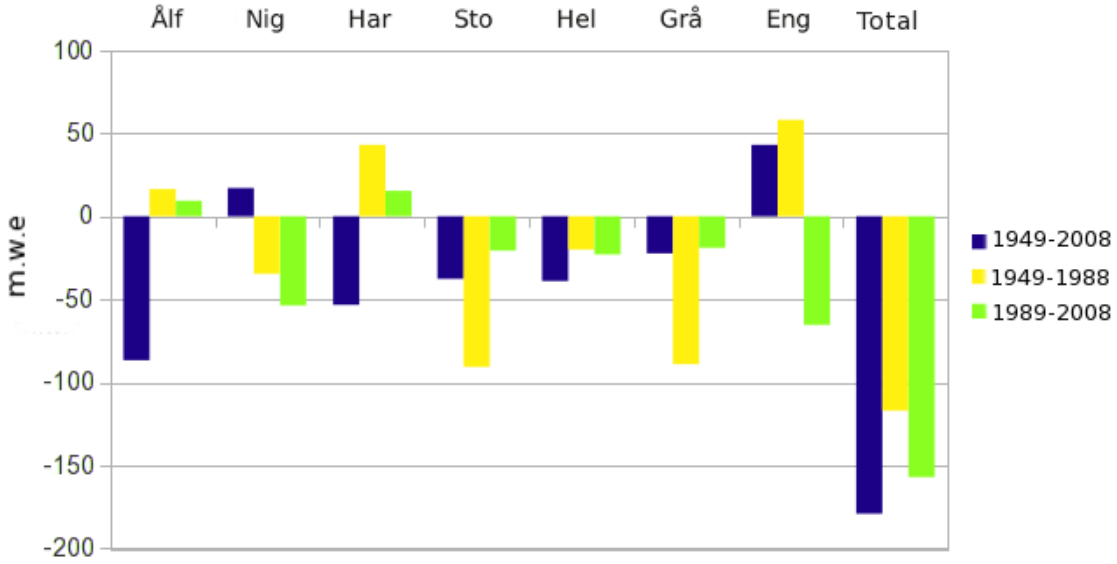

Figure 5.4: Multi-model ensemble means of cumulative net mass balance estimates at the end of the 2000-2100 time period averaged over greenhouse gas emission scenarios for individual glaciers and the sum.

The value of the net balance estimates show a greater sensitivity to the training time periods for the regression model than to the different emission scenarios. Averaging over greenhouse gas emission scenarios, the sum of the mean estimates are -179 m.w.e., -117 m.w.e. and -157 m.w.e. for the model training time periods 1949-2008, 1949-1988 and 1989-2008 respectively (Fig. 5.4). Averaging over the model training time periods, the sum of the mean estimates are -146 m.w.e., -167 m.w.e. and -139 m.w.e. for scenarios B1, A1B and A2 respectively (Fig. 5.5). The sum of the net mass balances of the glaciers in 2100 is negative for all regression models and scenarios. Out of the six glaciers lying on a similar latitude, the three most

continental glaciers, i.e. Gråsubreen, Hellstugubreen and Storbreen, are predicted to have a negative net mass balance in all cases. The net mass balance estimates for the three glaciers located closer to the coast and on similar latitudes, i.e. Ålfotbreen, Nigardsbreen and Hardangerjøkelen are more ambivalent. The net mass balance estimates for Engabreen are the most positive according to the models trained in the 1949-2008 and 1949-1988 time period, but the most negative according to the models trained in the 1989-2008 time period.

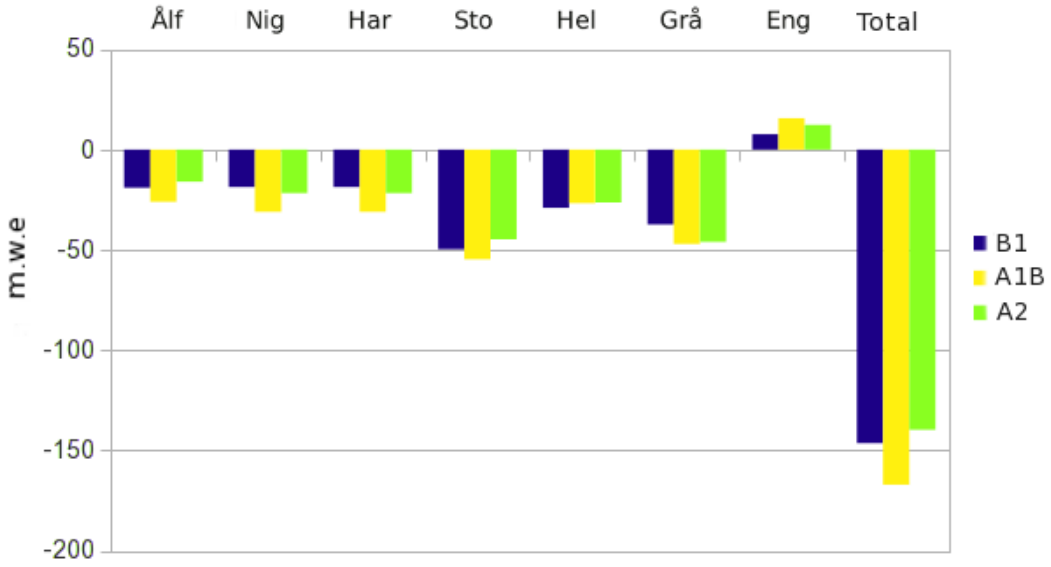

Figure 5.5: Multi-model ensemble means of cumulative net mass balance estimates at the end of the 2000-2100 time period averaged over model training time period for individual glaciers and the sum.

6 Bayesian Assessment of Modelled Climates in View of Observed Atmospheric States

This chapter describes the results of the Bayesian classification procedure described in section 3.5. The investigation was carried out with the predictors of the first predictor set comprised of the PC scores of the leading five principal components of PCA$_{NA}$ and the spatiotemporal means of precipitation rates and temperatures. The categories used for this classification are five 30 year time periods of modelled climate. These include two present-day time periods (1951-1980 and 1981-2010) and three future time periods (2011-2040, 2041-2070 and 2071-2100).

6.1 Probabilities of Modelled Climates in View of Observed Atmospheric States of Individual Years

This section presents the posterior probabilities of the time periods m_i of modelled climate in view of the observed state of the atmosphere for every individual year in the present-day time span of 1949-2008. For the summer season, the posterior probabilities for the two present-day time periods (~0.2) do not change significantly with the substitution of the data vector $\boldsymbol{d}$ for each year (Fig. 6.1 top). The probability of the climate state in the most distant future increases for the observed atmospheric states of more recent years. The posterior probabilities calculated for the winter season (Fig. 6.1 bottom) do not show any significant trends over the time span of observations. For 15 specific years, the data vector $\boldsymbol{d}$ produces high

posterior probabilities for one or both of the present-day time periods. However, for other years the posteriors for all categories are typically within a 0.2 ± 0.1 interval and therefore do not not deviate much from the equally distributed prior probabilities.

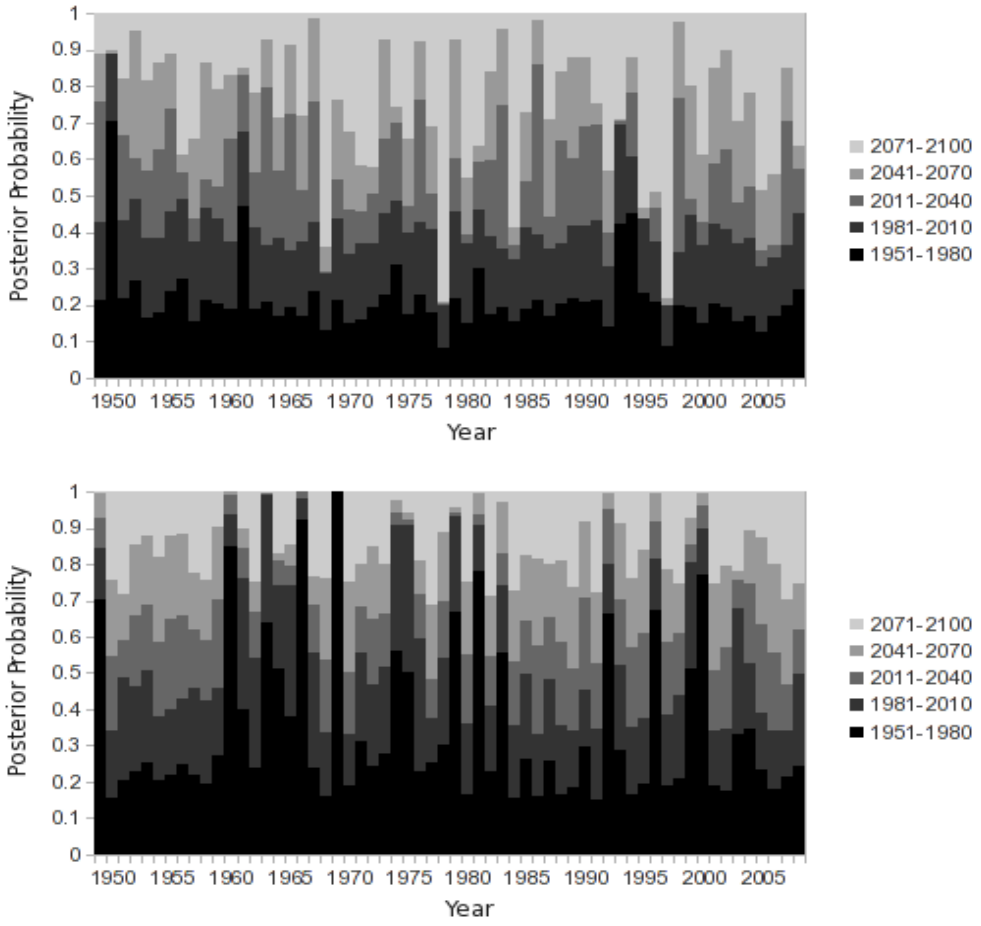

Figure 6.1: Posterior probabilities for climates of different future time periods for the observation data vector of summer (top) and winter (bottom) of each year.

6.2 Probabilities of Modelled Climates in View of Observed Atmospheric States of Composites of Years

This section presents the posterior probabilities of the time periods m_i of modelled climate in view of the observed mean state of the atmosphere for different composites of years in the present-day time span of 1949-2008.

6.2.1 Probabilities for Years of Highly Positive Mass Balance

The posterior probabilities for composites of years marked by most positive glacial mass changes are presented. In the winter season, these are the years in which the glaciers gained most mass. In the summer season, they are years characterised by the smallest loss of mass.

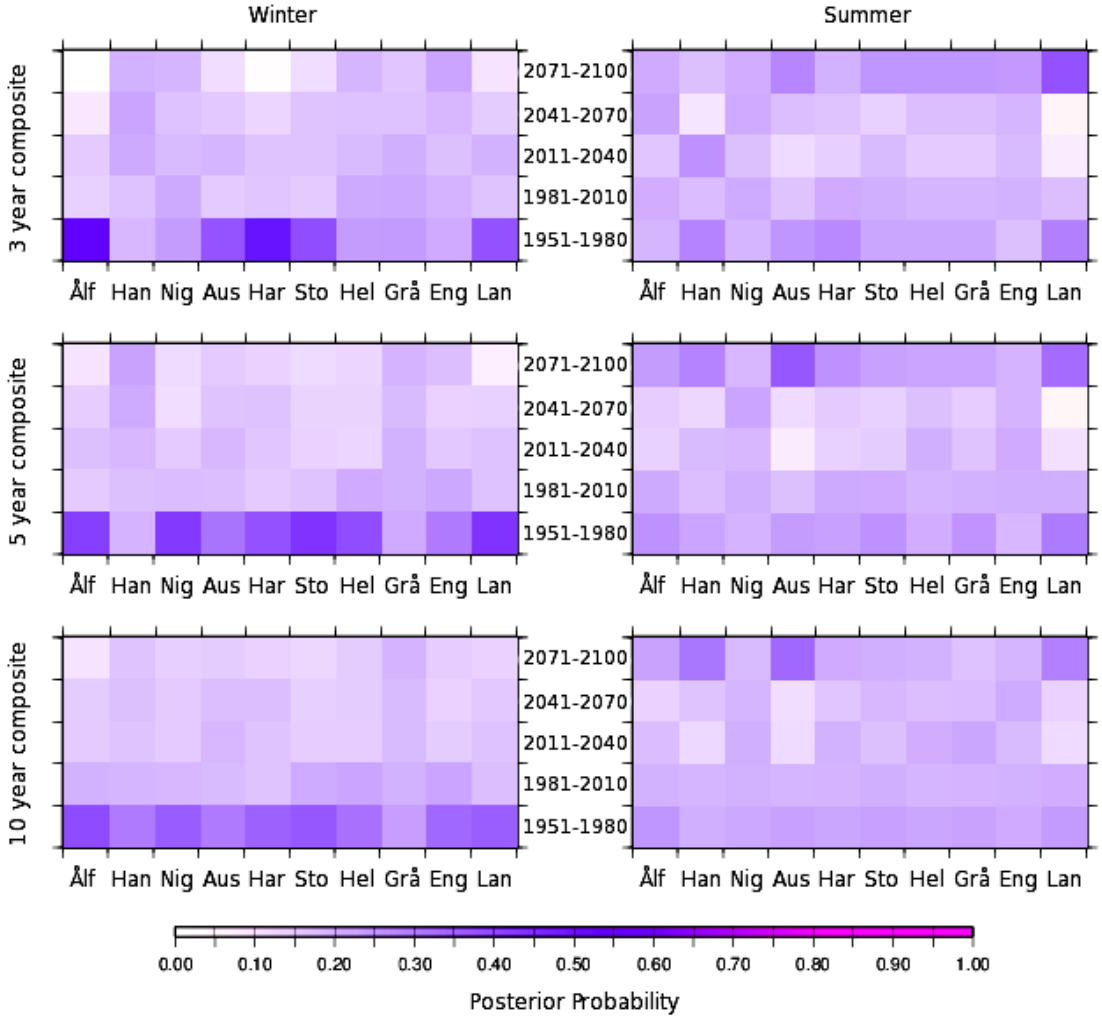

Figure 6.2: Posterior probabilities for climates of different future time periods for different glaciers, winter (left) and summer (right) in view of the composites of years characterised by most positive mass balance.

For the winter season, the posterior probabilities for the time period 1951-1980 are typically the highest, while there is no significant difference between the posteriors of the other categories (Fig. 6.2, left). Exceptions are evident for the glaciers Hansebreen, Nigardsbreen, Hellstugubreen, Gråsubreen and Engabreen in the analysis using 3-year composites, for Hansebreen and Gråsubreen in the analysis using 5-year composites, and for Gråsubreen in the analysis using 10-year composites. The general pattern can be observed for more glaciers as the number of years included in the construction of the composites increases. However, this also results in a decrease in the intensity of the pattern.

For the summer season, there is no apparent pattern in the posterior probabilities for most glaciers (Fig. 6.2, right). Exceptions are evident for the glaciers Hansebreen, Austdalsbreen and Langfjordjøkelen. The posteriors calculated for the time period in the most distant future are highest for Austdalsbreen and Langfjordjøkelen in the analyses using the 5-year and 10-year composites. The posteriors calculated for Hansebreen show a similar, but weaker pattern in the analyses using the 5-year and 10-year composites.

6.2.2 Probabilities for Years of Highly Negative Mass Balance

The posterior probabilities for composites of years characterised by most negative glacial mass changes are presented. In the winter season, these are the years in which the glaciers gained the least amount of mass. In the summer season, they are years in which the glaciers experience the greatest loss of mass.

For the winter season, the posterior probabilities for the time period 1951-1980 are typically the highest, while there is no significant difference between the posteriors of the other categories (Fig 6.3, left). Exceptions are evident for the glaciers Hansebreen and Engabreen in the analysis using 3-year composites and for the Engabreen in the analysis using 5-year composites. The general pattern can be observed for more glaciers as the number of years included in the construction of the composites increases. However, this also results in a decrease in the intensity of the patterns.

For the summer season, the posterior probabilities for the time period in the most distant future are typically the highest, while there is no significant difference between the posteriors of the other categories (Fig 6.3, right). Exceptions are evident for the glaciers Ålfotbreen, Hansebreen, Nigardsbreen and Engabreen in the analysis using 3-year composites and for Ålfotbreen and Hansebreen using 5-year composites. The general pattern can be observed for more glaciers as the number of years included in the construction of the composites increases. However, this also results in a decrease in the intensity of the pattern.

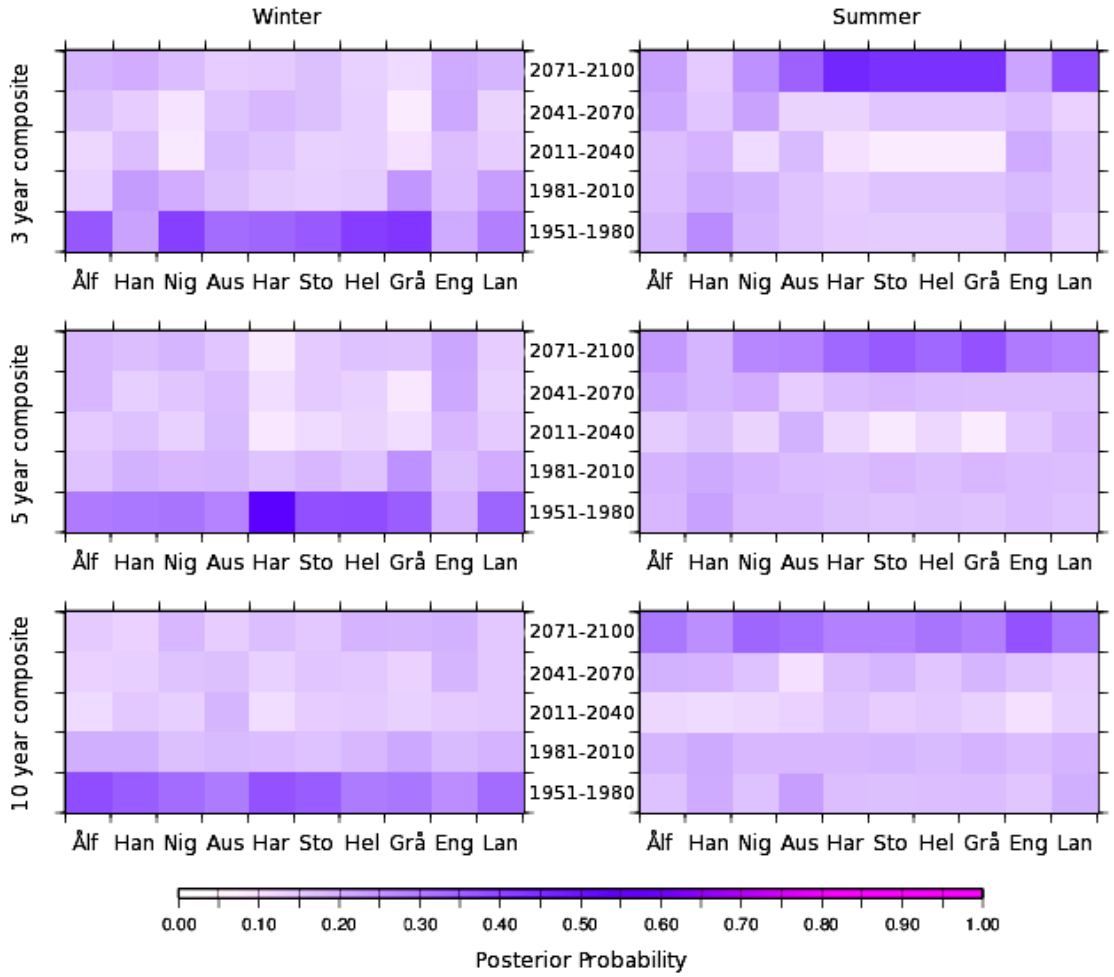

Figure 6.3: Posterior probabilities for climates of different future time periods for different glaciers, winter (left) and summer (right) in view of the composites of years characterised by most negative mass balance

7 Summary and Discussion

This final chapter summarises the findings described in chapters 4,5 and 6 and discusses these in context of related research in order to assess the way in which this study complements previous studies and contributes to the understanding of present-day glacier-climate dynamics and future changes of glacier mass balance in Norway. Additional notes are made about the shortcomings of the study and the need for further research.

In chapters 4, the atmospheric variables constructed from NCEP/NCAR re-analyses, the results of the correlation analyses between glacier mass balances and the variables constructed from NCEP/NCAR and ERA40 data, and the results of the cross-validated stepwise multiple regression analysis are presented. The regional winter precipitation rates and summer air temperatures averaged over the six months periods (ONDJFM, AMJJAS) that roughly correspond to the accumulation and ablation periods and mass balance measurement intervals (ANDREASSEN et al., 2011) correlate higher with the mass balance than the regional precipitation rates and air temperatures averaged over the three month seasons DJF and JJA. The highest *r* values from winter mass balance and spatiotemporal means of both NCEP/NCAR and ERA40 are obtained for the time period 1989-2008. Furthermore, the Pearson *r* values decrease with an increase in degree of continentality of the glaciers in all considered time periods. The same patterns are evident for *r* values calculated from correlation analyses with spatiotemporal means of both NCEP/NCAR and ERA40 air temperature, and the PC scores of the first PC of PCA$_{NA}$(w), PCA$_{NH}$(w) and PCA$_{STP2}$(w). In most cases, the spatiotemporal means constructed from NCEP/NCAR re-analyses describe the winter and summer mass balance better than the corresponding means constructed from ERA40 re-analyses. The winter

North Atlantic Oscillation (NAO) and Arctic Oscillation (AO) or Northern Annular Mode (NAM) variability described by the principal components of the various PCAs correlate more with the glacier winter mass balance than the three stationary NAO indices. The highest *r* values for the winter season are obtained from the first PC of PCA$_{NA}$(w) (0.88), i.e. the NAO, followed by the first PC of PCA$_{NH}$(w), i.e. the AO or NAM. These are highest for the 1989-2008 time period. In most cases, the NAO and NAM show a stronger correlation than the precipitation means, suggesting they represent the precipitation relevant to mass accumulation in winter better than regional means of NCEP/NCAR and ERA40 precipitation. According to the results of the multiple regression analyses carried out with winter mass balances and the three different sets of predictors, the NAO, NAM and NAO-like variable of the third set are the most dominant predictors in time periods 1949-2008 and 1989-2008. In most cases, these predictors explain more of the mass balance variance of maritime glaciers and the amount of explained variance decreases with an increase in the degree of continentality of the glaciers. The time period 1989-2008 has the highest explained winter mass balance variances overall. In summary, the dynamic NAO and related indices contribute most to the explained winter accumulation. The negative and positive phases of the NAO are associated with changes in the strength and location of the North Atlantic jet stream and shifts in zonal and meridional heat and moisture transport (HURRELL 1995). This modifies temperature and precipitation patterns on a large scale that may extend from Europe to North America (WALKER and BLISS 1932, VAN LOON and ROGERS 1978, ROGERS and VAN LOON 1979, NOAA-CPC, 2012). The positive phase, characterised by low pressure anomalies over Iceland and high pressure anomalies at the Azores, is associated with higher temperatures and precipitation in northern Europe. This is consistent with the eigenvector loadings of the first PC of PCA$_{STP2}$(w) that show a covariance of a positive phase NAO pattern with elevated temperatures and precipitation rates in southern Norway. Since the 1980's the winter NAO has predominantly been in a positive phase (HURREL and VAN LOON, 1997). Taking into consideration the previous investigations linking the wet and mild winters caused by the NAO to mass balance

changes in Scandinavia (e.g. SIX et al., 2001; NESJE and DAHL, 2003, NESJE et al., 2000), this NAO phase extreme may explain the particularly strong correlation between winter mass balance and the NAO index and the high explained variances in the 1989-2008 time period. Following the NAO- and AO/NAM indices and spatiotemporal air temperature and precipitation rate means, the highest correlation coefficients for the winter season are obtained from the analyses with the PC scores of the second PC of PCA$_{NA}$(w). Its eigenvector loadings show similarity to the Scandinavia pattern (SCAND) that has also been referred to as the Eurasia-1 pattern by BARNSTON and LIVEZEY (1987). The SCAND time series also significantly contributes to the explained variance calculated by the multiple regression carried out for the time period 1989-2008 with the second predictor set. The positive phase of the Scandinavia pattern is associated with negative temperature anomalies in central Russia and western Europe, positive precipitation anomalies in central and southern Europe and negative precipitation anomalies across Scandinavia (BARNSTON and LIVEZEY, 1987, NOAA-CPC, 2012). The below-average winter precipitation might explain the negative correlation of the SCAND time series and glacier winter mass accumulation.

In the correlation analyses carried out for the ablation season, the highest correlation coefficients were obtained from six months spatiotemporal means of both NCEP/NCAR and ERA40 air temperature. Unlike the Pearson *r* values from winter temperature, precipitation and NAO- and NAO-like indices, these show no pattern of increase or decrease with changing degrees of continentality of the glaciers. Nevertheless, the highest correlation coefficients are obtained from the winter mass balance of the maritime Ålfotbreen. The temperature means contribute to virtually all explained variance of summer glacier mass loss in multiple regression carried out with the second predictor set for the time periods 1949-2008 and 1989-2008. On average, temperature explains most of the mass loss variance in the latter time period. According to the results of the multiple regression analyses carried out with the first predictor sets, the PC scores of the third and fifth PC of PCA$_{NA}$(s) contribute most to the explained glacier summer mass balance variance in time period 1949-2008, while the

PC scores of the second PC of PCANA(s) contributes most to the explained summer mass balance variance in the time period 1989-2008. The results from the multiple regression analyses carried out with the third predictor sets show that the PC scores of the second PC of PCASTP2(s) contribute most to the explained glacier summer mass balance variance in time periods 1949-2008 and 1989-2008. On average, the second PC of PCASTP2(s) explains more of the summer mass balance variance in 1949-2008 and 1989-2008 than others. The eigenvector loadings of the second PC of PCASTP2(s) showed a covariance of the sea level pressure pattern and temperature over southern Norway and resembles the summer Scandinavia pattern. The positive phase of this teleconnection pattern is characterised by high sea level pressure over South-East Scandinavia, sometimes reflecting major blocking highs (BARNSTON and LIVEZEY, 1987, NOAA-CPC, 2012). In summer it is associated with increased precipitation and low temperatures in central Europe and reduced precipitation and elevated temperatures in Scandinavia (NOAA-CPC, 2012), which may explain the importance of this predictor.

The correlation coefficients calculated from moving 10 year time windows of the winter NAO index and glacier winter mass balance change from low, statistically insignificant R values to correlation coefficients between 0.6 and 0.95 in the mid 1980's. This change point suggests that the NAO variability might overshadow the influence of other factors on the winter mass balance during the time period in which the NAO is in an extreme positive phase. Glaciers underlying a continental regime show a weaker response to the increase in NAO index values than the maritime glaciers. The change point in net glacier mass balance (e.g. FEALY and SWEENEY, 2005) takes place in the late 1980's while the sudden increase in correlation coefficients calculated from the winter NAO index and winter mass balance takes place in the early 1980's. The change point in the late 1980's coincides with particular low regional summer temperatures in southern Norway. While the summer temperatures rise again in subsequent years, the winter NAO also becomes more positive and the precipitation precipitation increases, presumably counteracting the once again high mass loss in summer and ultimately resulting in a more positive net mass

balance. After the year 2000, which marks the beginning of a rapid loss in glacier mass (e.g. ANREASSEN et al., 2008), the NAO index values decrease, but remain high in comparison to the values in the 1950's and 1960's, and the high correlation between the winter NAO and winter mass balance prevails for all glaciers except Engabreen and Gråsubreen. At the same time, the regional summer temperature in southern Norway rises and sets new record highs for the investigated time period. These changes are accompanied by a decrease in winter accumulation and strong increase in mass loss during the ablation season, resulting in overall negative net mass balances. Only Ålfotbreen is excluded from this scale of annual mass loss since 2000. In summary, the net glacier mass surplus in the 1980's and 1990's may be attributed to a combination of the increased precipitation due to the predominantly positive NAO and the relatively low ablation season temperatures during that time. This is consistent with findings of previous studies (e.g. CHINN et al., 2005; RASMUSSEN et al., 2007). The annual mass deficit since the year 2000 may be attributed to the weakening in the winter NAO causing less accumulation in winter, and the increase in ablation season temperatures resulting in unprecedented summer melting.

The correlation coefficients calculated from moving 10 year windows of glacial summer mass balance and spatiotemporal means of air temperature in the ablation season shift from high negative values in the 1970's to positive values in the 1980's and 1990's and return to slightly negative values in the 2000's. This suggests that the regional means temperature do not represent the temperatures directly relevant to melting in the 1980's and 1990's as in the 1970's and 2000's and supports the idea of the regime shift discussed in the previous paragraph.

In conclusion, the precipitation relevant to glacier mass accumulation in winter is described better by the dynamic NAO and NAM index values from principal component analyses than by regional means of precipitation or any other atmospheric variable constructed from the NCEP/NCAR and ERA40 re-analysis in this study. When the winter NAO enters its extreme phase in the 1980's and 1990's, this relationship is strengthened. Furthermore, there is an East-West gradient in the strength of relationship between mass accumulation in winter and the NAO and NAM. There is no

such apparent gradient of the influence of temperature on summer melting. These aspects of the glaciological regimes of the investigated glaciers might explain why the mass surplus in the late 1980's and 1990's is particularly pronounced for the maritime glaciers such as Ålfotbreen, less evident for the intermediate Storbreen and only expressed as a temporary halt in net mass loss of the most continental glaciers Hellstugubreen and Gråsubreen. Given that the glaciological regime is defined by the meteorological and regional geographic influences the glacier is subject to, the different reactions of the glaciers to the change in the NAO may also be viewed as a result of differences in the glaciological regime. The temperature relevant to summer melting of glaciers is best described by the second principal component of the PCA$_{STP2}$, which shows resemblance to the summer Scandinavia pattern and associated temperatures. Overall, the atmospheric variables constructed in this study better describe the meteorological aspects of the glaciological regime in the more recent decades of the investigated total time period.

In chapters 5, the results of the application of the multiple regression model trained with the first predictor set to the variables reconstructed from interpolated CMIP3 climate model output are presented. The estimated for winter accumulation and summer melting is generally greatest for the most maritime glaciers. Estimates of a significant positive trend of mass accumulation in winter of maritime glaciers can be seen for model simulations that predict a positive NAO trend that would be consistent with the projected development of the NAO and AO under global warming (FYFE et al., 1999). Summer melting is greater according to estimates from simulations for the A2 and A1B emission scenario than for the B1 scenario. According to most estimates, summer melting increases over the 2000-2100 time period. Multi-model ensemble cumulative net mass balance estimates range from a ~50 m.w.e. mass surplus to a ~100 m.w.e. mass deficit. These estimates reveal a greater sensitivity to the training time period of multiple regression model than to the emission scenarios. At the end of the 2000-2100 time period, the three more eastern glaciers Gråsubreen, Hellstugubreen and Storbreen, show a net mass

deficit for all scenarios and model training time period. Averaged over the emission scenarios, the sums of the mean estimates generated in this study range from -117 m.w.e. (for model training time period 1949-1988) to -179 m.w.e. (for model training time period 1949-2008). Averaged over model training time periods, the sums of the mean estimates range from -139 m.w.e. (for the A2 emission scenario) to 167 m.w.e. (for the A1B emission scenario). The estimates for the three more western glaciers Ålfotbreen, Hardangerjøkelen and Nigardsbreen are more ambivalent. Out of these glaciers, the greatest mass deficits glaciers are estimated for Ålfotbreen by the model trained in the 1949-2008 time period and Nigardsbreen for the time periods 1949-1988 and 1989-2008. These extremes coincide with the link of their summer melting to temperature means in the multiple regression models. The PC scores of the second PC of PCA$_{NA}$(s), the otherwise dominant predictor in the ablation season, correlates with the temperature predictor in over a number of time periods, e.g. r=~ -0.5 for 1955-1975, making them 'competing' predictors in the multiple regression model due to the measures taken to prevent overfitting and to ensure the robustness of the model. In the multiple regression analysis using the second predictor set, temperature is the dominant predictor in the ablation season. This both demonstrates the robustness of temperature as a predictor and indicates the predictor choice of the regression model in absence of the correlated PC scores of the second PC of PCA$_{NA}$(s). In order to understand the ambivalent estimates for the maritime glaciers, the sensitivity of these to the selection of temperature as a main predictor in the ablation season could be investigated by removing the PC scores of the second PC of PCA$_{NA}$(s) from the first predictor set, thus suppressing the 'competition-effect' of multicollinearity, and generating the estimates from the resulting regression model.

In conclusion, the net mass balance estimates show a greater mass loss for the continental glaciers than for the maritime glaciers. This difference may be attributed to the choice of ablation season predictors or the strong relationship of the winter mass balance of maritime glaciers to the NAO, which might create increased winter accumulation to compensate for the mass loss in summer to some extend. The most northern glacier Engabreen

shows the greatest mass surplus in the 2000-2100 time span. The estimates are more sensitive to the model training time period than to greenhouse gas emission scenarios. The model training time periods in this study are chosen because of the presumably different prevailing glaciological regimes at those times. The multiple regression analyses in chapter 4 confirm this in the sense that different dominant predictors were often determined for these time periods. For example, the NAO was determined as the dominant predictor for all glaciers in the multiple regression analyses in the 1989-2008 time period, while it was only determined as the dominant predictor for one of the glaciers in the multiple regression analyses in the 1949-1988 time period. Therefore, the high sensitivity of mass balance estimates to the training time period of the models may also be viewed as the sensitivity of the development of mass changes to the prevailing glaciological regimes. Following the discussion of results of the fourth chapter, this may in turn be a function of the strength and phase of the NAO to some extent.

In chapters 6, the results of the Bayesian classification observed states of the atmosphere into time periods of modelled climate are presented. The temperature and precipitation means and PC scores of the leading five PCs of PCA$_{NA}$ are used to describe the present-day atmospheric states and future climates.

In the summer season, the posterior probabilities for the climate in the most distance future time period is higher in view of observed states of the atmosphere of individual years, suggesting that the most recent decades better represent the atmospheric summer conditions in a more distant future.

The posterior probabilities of modelled climates in view of the composites of years characterised by highest accumulation in winter are on average highest for the 1951-1980 climate and low for the climate in the most distant future. This is less pronounced for Hansebreen, Gråsubreen and Engabreen. This points towards distant future climatic conditions that generally favour strong winter accumulation less than the modelled climatic conditions of 1951-1980. The posterior probabilities of modelled

climates in view of the composites of summers characterised by minimal mass loss show a more even distribution over the different time periods and glaciers. This suggests little change in the climatic conditions that favoured least melting during the past ablation seasons. Langfjordjøkelen, Austdalsbreen and to a lesser extend Hansebreen are exceptions suggesting higher probabilities for climatic conditions favouring least summer melting during the ablation season in the most distant future.

The posterior probabilities of modelled climates in view of the composites of years characterised by least accumulation in winter are on average highest for the 1951-1980. This suggests distant future climatic conditions that favour minima of accumulation in winter less. The posterior probabilities of modelled climates in view of the composites of years characterised by most mass loss in the ablation season are on average highest for the modelled climate in the most distant future time period. This pattern is less pronounced for more western glaciers in coastal proximity and Engabreen. This suggests that the ablation season atmospheric conditions of modelled climate in the distant future favour more melting of most glaciers than atmospheric conditions of modelled climate in more recent time periods.

These interpretation of the trends of atmospheric conditions favouring these extremes in positive and negative mass change in the accumulation and ablation season are made under the assumption that the modelled climate of the 20th century adequately represents the actual climate. While the likelihood of observing these conditions in different modelled climates is unaffected by the correctness of this assumption and therefore the trend of posterior probabilities also exists in disregard of it, the correctness of the assumption has implications on the use of this trend in the extrapolation from observed present-day conditions. Furthermore, since the composites were constructed for each glacier individually, the interpretation of the pattern of posterior probabilities over the time periods of modelled climate must be put in context of the dynamics of the individual glaciers.

In conclusion, the atmospheric conditions of the modelled climate of the time period in the most distant future favour greater mass loss in the

ablation season, while both minima and maxima in mass change in the accumulation season become less probable, provided that modelled present-day climate adequately represents the actual climate. The higher probability of distant future atmospheric conditions favouring mass loss extremes in summer is in agreement with the estimated accelerated mass loss at the end of the 2000-2100 time period.

Bibliography

Andreassen, L.M., H. Elvehøy, M. Jackson, B. Kjøllmoen, R.V. Engeset, R.H. Giesen, 2011: Glaciological investigations in Norway in 2010. Report 3/2011. - Norges Vassdrags- og Energidirektoratet, Oslo.

Andreassen, L.M., H. Elvehøy, B. Kjøllmoen, R.V. Engeset, N. Haakensen, 2005: Glacier mass-balance and length variation in Norway. - Annals of Glaciology **42**, 317-325.

Andreassen, L.M., J. Oerlemans, 2009: Modelling long-term summer and winter balances and the climate sensitivity of Storbreen, Norway. - Geografiska Annaler **91**(4), 233-251.

Andreassen, L.M., F. Paul, A. Kaab, J.E. Hausberg, 2008: Landsat-derived glacier inventory for Jotunheimen, Norway, and deduced glacier changes since the 1930s. - Cryosphere **2,** 131-145.

Bahrenberg, G., E. Giese, J. Nipper, 1999: Statistische Methoden in der Geographie, Band 1 Univariate und bivariate Statistik. - Teubner Studienbuecher der Geographie, Stuttgart, Leipzig, 236.

Bahrenberg, G., E. Giese, N. Mevenkamp, J. Nipper, 2008: Statistische Methoden in der Geographie, Band 2 Multivariate Statistik. - Studienbuecher der Geographie, Stuttgart, 386.

Bakke, J., S.O. Dahl, A. Nesje, 2005: Lateglacial and early Holocene palaeoclimatic reconstruction based on glacier fluctuations and equilibrium-line altitudes at northern Folgefonna, Hardanger, western Norway. - Journal of Quarternary Science **20**, 1-20.

Bamber, J.L., A. Payne (Eds), 2004: Mass balance of the cryosphere. In: Observations and modelling of contemporary and future changes. - Cambridge University Press, Cambridge, New York, Melbourne, 644.

Barnston, A.G., R.E. Livezey, 1987: Classification, Seasonality and Persistence of Low-Frequency Atmospheric Circulation Patterns. - Monthly Weather Review **115**(6), 1083-1126.

Barry, R., 2006: The status of research on glaciers and global glacier recession: a review. - Progress in Physical Geography **20**, 285.

Berger, J.O., 1985: Statistical Decision Theory and Bayesian Analysis. - Springer, New York, Berlin, 617.

Berliner, L.M., R.A. Levine, D.J. Shea, 2000: Bayesian climate change assessment. - Journal of Climate **13**, 3805-3820.

Bjune, A.E., J. Bakke, A. Nesje, H.J.B. Birks, 2005: Holocene mean July temperature and winter precipitation in western Norway inferred from palynological and glaciological lake-sediment proxies. - The Holocene **15**, 177-189.

Braithwaite, R.J., Y. Zhang, 1999: Modelling changes in mass balance that may occur as a result of climate changes. - Geografiska Annaler **81** A(4), 489-496.

Caldeira, K., A. Jain, M. Hoffert, 2003: Climate sensitivity uncertainty and the need for energy without CO2 emissions. - Science **299**, 2052-2054.

Chinn, T., S. Winkler, M.J. Salinger, N. Haakensen, 2005: Recent glacier advances in Norway and New Zealand: A comparison of their glaciological and meteorological causes. - Geogr. Ann. **87A**(1), 141-157.

Cubasch, U., D. Kasang, 2000: Anthropogener Klimawandel. - Klett-Perthes, Gotha, Stuttgart, 128.

D'Agostini, G., 2003: Bayesian inference in progressing experimental data: principles and basic applications. - Reports on Progress in Physics **66**(9), 1383-1419.

Dahl, S.O., A. Nesje, 1994: Holocene glacier fluctuations at Hardangerjøkulen, central-southern Norway: a high resolution composite chronology from lacustrine and terrestrial deposits. - The Holocene **4**, 269–277.

Dahl, S.O., A. Nesje, 1996: A new approach to calculating Holocene winter precipitation by combining glacier equilibrium-line altitudes and pine-tree limits: a case study from Hardangerjøkulen, central southern Norway. - The Holocene **6**, 381–398.

Dyurgerov, M., 2003: Mountain and subpolar glaciers show an increase in sensitivity to climate warming and intensification of the water cycle. - Journal of Hydrology **282**, 164–176.

Dyurgerov, M., 2005: Mountain glaciers are at risk of extinction. - In: Huber, U.M., Bugmann, H. K. M. and Reasoner (Eds.), Global Change in Mountain Regions. Springer, The Netherlands, 177–185.

Dyurgerov, M., M. Meier, 2000: Twentieth century climate change: Evidence from small glaciers. - Proceedings of the National Academy of Sciences of the United States of America **97**, 1406-1411.

Earth System Research Laboratory, 2011: NCEP/NCAR Reanalysis 1: Summary.
http://www.esrl.noaa.gov/psd/data/gridded/data.ncep.reanalysis.html,
last accessed on 13.12.2011.

ECMWF, 2012: ERA 40 year re.analysis, monthly means of daily means. http://data-portal.ecmwf.int/data/d/era40_moda/,
last accessed on 20.02.2012.

Fealy, R., J. Sweeney, 2005: Detection of a possible change point in atmospheric variability in the North Atlantic and its effects on Scandinavian glacier mass balance. - International Journal of Climatology **25**, 1819-1833.

Friedrichs, P., H. Paeth, 2006: Seasonal prediction of African precipitation with ECHAM4-T42 ensemble simulations using a multivariate MOS re-calibration scheme. - Climate Dynamics **27**, 761-786.

Fyfe J.C., G.J. Boer, G.M. Flato, 1999: The Arctic and Antarctic Oscillations and their projected changes under global warming. - Geophysical Research Letters **26**, 1601-1604.

Gibson, R., P. Kallberg, S. Uppala, A. Hernandez, A. Nomura, E. Serrano, 1997: ERA description. Reanalysis Project Report Series No. 1. European Centre for Medium-Range Weather Forecasts (ECMWF).

Giorgi, F., E. Coppola, 2009: Projections of twenty-first century climate over Europe. – The European Physical Journal Conferences **1**, 29–46.

Glahn, H., D. Lowry, 1972: The Use of Model Output Statistics (MOS) in Objective Weather Forecasting. – Journal of Applied Meteorology **11**, 1203–1211.

Greuell, J.W., J. Oerlemans, 1989: Energy balance calculations on and near Hintereisferner (Austria) and an estimate of the effect of greenhouse warming on ablation. - In: Oerlemans, J. (Ed), Glacier fluctuations and climatic change, Reidel, Dordrecht, 235-260.

Greuell, J.W., 1989: Glaciers and climate: energy balance studies and numerical modelling of historical front variations of the Hintereisferner (Austria). - Dissertation, University of Utrecht.

Guisan, A., J.I. Holten, R. Spichinger, L. Tessier, 1995: Potential impacts of climate change in the Alps and Fennoscandian mountains. - UNESCO, Genf.

Haeberli, W., M. Beniston, 1998: Climate change and its impact on glaciers and permafrost in the Alps. - Ambio **27**, 258-265.

Haeberli, W., R. Frauenfelder, M Hoelzle, M. Maisch, 1999: On rates and acceleration trends of global glacier mass changes. - Geografiska Annaler **81A**, 585-591.

Haeberli, W., M Hoelzle, M. Maisch, 1998: Gletscher – Schlüsselindikatoren der globalen Klimaänderung. - In: Lozàn, J.L., H. Grassl, H. Hupfer, Warnsignal Klima – Wissenschaftliche Fakten. Wissenschaftliche Auswertung, Hamburg, 213-221.

Haeberli, W., M. Hoelzle, F. Paul, M. Zemp, 2007: Integrated monitoring of mountain glaciers as key indicators of global climate change: The European Alps. - Annals of Glaciology **31**, 241-246.

Haeberli, W., H.J. Zumbühl, 2003: Schwankungen der Alpengletscher im Wandel von Klima und Perzeption. - Jahrbuch der Geographischen Gesellschaft Bern **61/2003**, 77-92.

Hasselmann, K., 1998: Conventional and Bayesian approach to climate-change detection and attribution. - Quarterly Journal of the Royal Meteorological Society **124(**552), 2541-2565.

Hoelzle, M., T. Chinn, D. Stumm, F. Paul, M. Zemp, W. Haeberli, 2007: The application of glacier inventory data for estimating past climate change

effects on mountain glaciers: A comparison between the European Alps and Southern Alps of New Zealand. - Global and Planetary Change **56**, 69-82.

Hoelzle, M., M. Dischl, R. Frauenfelder, 2000: Weltweite Gletscherbeobachtung als Indikator der globalen Klimaänderung. - Vierteljahrsschrift der Naturforschenden Gesellschaft Zürich **145**(1), 5-12.

Houghton, J.T., Y. Ding, D.J. Griggs, M. Noguer, P.J. Van der Linden, X. Dai, K. Maskell, C.A. Johnson, 2001: Climate change 2001. The Scientific Basis. Cambridge University Press, Cambridge, 944.

Huber U.M., M.A. Reasoner, H. Bugmann (eds), 2005: Global change and mountain regions – a state of knowledge and overview. - Kluwer, Dordrecht.

Hurrell, J., 1995: Decadal trends in the North Atlantic Oscillation: regional temperatures and precipitation. – Science **269**, 676–679.

Hurrell, J., H. Van Loon, 1997: Decadal variations in climate associated with the North Atlantic Oscillation. - Climate Change **36**(3-4), 301-326

IPCC, 2007: Climate Change 2007: The Physical Science Basis. Contribution of Working Group I to the Fourth Assessment Report of the Intergovernmental Panel on Climate Change [Solomon, S., D. Qin, M. Manning, Z. Chen, M. Marquis, K.B. Averyt, M.Tignor and H.L. Miller (Eds.)]. - Cambridge University Press, Cambridge, United Kingdom and New York, USA.

Jacobeit, J., C. Beck, A. Philipp, 1998: Annual to decadal variability in climate in Europe - objectives and results of the German contribution to the European climate research project ADVICE. – Würzburger Geographische Manuskripte **43**, 163.

Jóhannesson, T., 1997: The response of two Icelandic glaciers to climatic warming computed with a degree-day glacier mass-balance model coupled to a dynamic glacier model. - Journal of Glaciology **43**, 321-327.

Jóhannesson, T. O. Sigurðsson, T. Laumann, M. Kennet, 1995: Degree-day glacier mass-balance modelling with applications to glaciers in Iceland, Norway and Greenland. - Journal of Glaciology **41**, 345-358.

Jones, P.D., T. Jónsson, D. Wheeler, 1997: Extension to the North Atlantic Oscillation using early instrumental pressure observations from Gibraltar and South-West Iceland. - International Journal of Climatology **17**, 1433-1450.

Kalnay, E., M. Kanamitsu, R. Kistler, W. Collins, D. Deaven, L. Gandin, M. Iredell, S. Saha, G. White, J. Woollen, 1996: The NCEP/NCAR 40-year reanalysis project. – Bulletin of the American Meteorological Society **77**(3), 437–471.

Kistler, R., W. Collins, S. Saha, G. White, J. Woollen, E. Kalnay, M. Chelliah, W. Ebisuzaki, M. Kanamitsu, V. Kousky, H. Van den Dool, R. Jenne, M. Fiorino, 2001: The NCEP−NCAR 50−Year Reanalysis: Monthly Means CD−ROM and Documentation. – Bulletin of the American Meteorological Society **82**(2), 247–267.

Krishnamurti, T. N., C. M. Kishtawal, T. E. LaRow, D. R. Bachiochi, Z. Zhang, C. E Williford, S. Gadgil, S. Surendran, 1999: Improved weather and seasonal climate forecasts from multimodel superensemble. - Science **285**, 1548-1550.

Kuhn, M., E. Dreiseitl, S. Hofinger, G. Markl, N. Span, N. Kaiser, 1999: Measurements and models of the mass balance of Hintereisferner. - Geografiska Annaler **81**A, 659-670.

Laumann, T., 1992: Simulering av breers massebalanse. Publikasjon 1992/17 - Norges Vassdrags- og Energidirektoratet, Oslo.

Laumann, T., N. Reeh, 1993. Sensitivity to climate change of the mass balance of glaciers in southern Norway. - Journal of Glaciology **39**, 329-346.

Landman, W.A., L. Goddard, 2002: Statistical Recalibration of GCM Forecasts over Southern Africa Using Model Output Statistics. - Journal of Climate **15**, 2038-2055.

Leroy, S., 1998: Detecting climate signals: some Bayesian aspects. - Journal of Climate **11**, 640-651.

Löffler, H., 1988: Natural hazards and health risks from lakes. - International Journal of Water Resources Development **4**(4), 276-283.

Maisch, M., 2002: Klimawandel und Gletscher. - Geographie heute **23**(203), 30-34.

Maisch, M., W. Haeberli, 2003: Die rezente Erwährmung der Atmosphäre – Folgen für die Schweizer Gletscher. - Geographische Rundschau **55**(2), 4-12.

Marshall, S.J., 2006: Modelling glacier response to climate change. - In: Knight, P.G., Glacier science and environmental change, Blackwell, Oxford, 163-173.

Meehl, G., C. Covey, T. Delworth, M. Latif, B. McAvaney, J. Mitchell, R. Stouffer, K. Taylor, 2007: The WCRP CMIP3 multi-model dataset: a new era in climate change research. - Bulletin of the American Meteorological Society **88**, 1383-1394

Michaelsen, J., 1987: Cross-validation in statistical climate forecast models. – Journal of Climate and Applied Meteorology **26**(11), 1589–1600.

Min, S., A. Hense, H. Paeth, W.-T. Kwon, 2004: A Bayesian decision method for climate change signal analysis. - Meteorologische Zeitschrift **13**(5), 421-436.

Nakicenovic, N., 2000: Greenhouse gas emissions scenario. - Technological Forecasting and Social Change, **65**, 149-166.

Nakicenovic, N., R. Swart, 2000: Emissions Scenarios – Cambridge University Press, Cambridge, UK.

Nesje, A., 1989: Glacier-front variations at the outlet glaciers from Jostedalsbreen and climate in the Jostedalsbre region of western Norway in the period 1901-1980. - Norsk Geografisk Tidsskrift **43**, 3-17.

Nesje, A., 1995: Breene i Vest-Norge vokser med rekordfart. - Naturen **119**, 7-10.

Nesje, A., 2005: Brisdalsbreen in western Norway: AD 1900-2004 frontal fluctuations as a combined effect of variations in winter precipitation and summer temperature. - The Holocene **15**(8), 1245-1252.

Nesje, A., J. Bakke, S.O. Dahl, Ø. Lie, J.A. Matthews, 2008: Norwegian mountain glaciers in the past, present and future. - Global and Planetary Change **60**, 10-27.

Nesje, A., S.O. Dahl, 2000: Glaciers and environmental change. - Arnold, London.

Nesje, A., S.O. Dahl, 2003: The 'Little Ice Age' – only temperature? - The Holocene **13**(1), 139-145.

Nesje, A., T. Jóhannesson, H.J.B. Birks, 1995: Briksdalsbreen, western Norway: climatic effects on the terminal response of a temperate glacier between AD 1901 and 1994. - The Holocene **5**, 343-347.

Nesje, A., Ø. Lie, S.O. Dahl, 2000: Is the North Atlantic Oscillation reflected in Scandinavian glacier mass balance records? - Journal of Quaternary Science **15**, 587-601.

Nesje, A., J. A. Matthews, S. O. Dahl, M. S. Berrisford, C. Andersson, 2001: Holocene glacier fluctuations of Flatebreen and winter-precipitation changes in the Jostedalsbreen region, western Norway, based on glaciolacustrine sediment records. - Holocene **11**, 267-280.

NOAA-CPC, 2012: Northern Hemisphere Teleconnection Patterns. NOAA National Weather Service Climate Prediction Center.
http://www.cpc.noaa.gov/data/teledoc/telecontents.shtml,
last accessed on 18.12.2012.

Nordli, Ø., Ø. Lie, A. Nesje, S.O. Dahl, 2003: Spring-summer temperature reconstruction in western Norway 1734-2003: A data-synthesis approach. - International Journal of Climatology **23**, 1821-1841.

Nordli, Ø., Ø. Lie, A. Nesje, R.E. Benestad, 2005: Glacier mass balance in southern Norway modelled by circulation indices and spring-summer temeratures AD 1781-200. - Geogr. Ann. **87**A(3), 431-445.

NVE, 2012. Norges vassdrags- og energidirektorat – Bre.
http://www.nve.no/no/Water/Hydrology/Glaciers/,
last accessed on 10.04.2013.

Oerlemans, J., 1986: An attempt to simulate historic front variations of Nigardsbreen. - Theoretical and Applied Climatology **34**, 126-135.

Oerlemans, J., 1988: Simulation of historic glacier variations with a simple climate-glacier model. - Journal of Glaciology **34**, 333-341.

Oerlemans, J., 1994: Quantifying global warming from the retreat of glaciers. - Science **264**, 243-245.

Oerlemans, J., 1997: A flowline model for Nigardsbreen, Norway: projection of future glacier length based on dynamic calibration with the historic record. - Annals of Glaciology **24**, 382-389.

Oerlemans, J., 2000: Holocene glacier fluctuations: is the current rate of retreat exceptional? - Annals of Glaciology **31**, 39-44.

Oerlemans, J., 2001: Glaciers and climate change. - Balkema, Rotterdam.

Oerlemans, J., 2005: Extracting a Climate Signal from 169 Glacier Records. - Science **308** 675-677.

Østrem G., M. Brugman, 1991: Glacier mass balance measurements. A manual for field and office work. National Hydrology Research Institute, Scientific Report, No.4. Environment Canada, N.H.R.I., Saskatoon and Norwegian Water Resources and Energy Directorate, Oslo, 224.

Østrem, G., N. Haakensen, 1993: Glaciers of Europe—glaciers of Norway. - In: Williams, R.S., Ferrigno, J.G. (Eds.), Satellite Image Atlas of Glaciers of the World. US Geological Survey Professional Paper 1386-E, US Geological Survey, Washington, E63–E109.

Østrem, G., Haakensen, N., Melander, O., 1973: Atlas over breer i Nord-Skandinavia [Atlas of glaciers in northern Scandinavia]: Meddelelse No. 22 fra Hydrologisk avdeling, Norges Vassdrags-og Elektrisitetsvesen, 315.

Østrem, G., K. D. Selvig, T. Tandberg, 1988: Atlas over breer i Sør-Norge [Atlas of glaciers in south Norway] (revised ed.): Meddelelse No. 61 fra Hydrologisk avdeling, Norges Vassdrags-og Energiverk, Oslo, 248.

Østrem, G., T. Ziegler, 1969: Atlas over breer i Sør-Norge [Atlas of glaciers in southern Norway]: Meddelelse No. 20 fra Hydrologisk avdeling, Norges vassdrags- og Elektrisitetsvesen, Oslo, 207.

Paeth, H. 2011: Postprocessing of simulated precipitation for impact research in West Africa. Part I: model output statistics for monthly data. - Climate Dynamics **36**, 1321-1336.

Paeth, H. R. Girmes, G. Menz, A. Hense, 2006: Improving seasonal forecasting in the low-latitudes. - Monthly Weather Review **134**, 1859–1879.

Paeth, H., A. Hense, 2003: Seasonal forecast of sub-sahelian rainfall using cross-validated model output statistics. - Meteorologische Zeitschrift **12**, 157-173.

Paeth, H., M. Rauthe, S. Min, 2007: Multi-model Bayesian assessment of climate change in the northern annular mode. - Global and Planetary Change **60**(3-4),193-206

Paeth, H., A. Scholten, P. Friedrichs, A. Hense, 2008: Uncertainties in climate change prediction: El Niño-Southern Oscillation and monsoons. - Global and Planetary Change **60**, 265-288.

Paul, F., L.M. Andreassen, S.H. Winsvold, 2011: A new glacier inventory for Jostedalsbreen region, Norway, from Landsat scenes of 2006 and changes since 1966. - Annals of Glaciology **52**, 153-162.

Pohjola, V.A., J.C. Rogers, 1997a: Atmospheric circulation and variations in Scandinavian glacier mass balance. - Quaternary Research **47**, 29-36.

Pohjola, V.A., J.C. Rogers, 1997b: Coupling between the atmospheric circulation and extremes of the mass balance of Storglaciären, northern Scandinavia. - Annals of Glaciology **24**, 229-233.

Radic, V., R. Hock, 2006: Modelling future glacier mass balance and volume changes using ERA-40 reanalysis and climate models: a sensitivity study at Storglaciären, Sweden. - Journal of Geophysical Research **111**, F 03003.

Rasmussen, L.A., L.M. Andreassen, H. Conway, 2007: Reconstruction of mass balance of glaciers in southern Norway back to 1948. - Annals of Glaciology **46**, 255-260.

Reichert, B.K., L. Bengtsson, J. Oerlemans, 2001: Midlatitude Forcing Mechanisms for Glacier Mass Balance Investigated Using General Circulation Models. - Journal of Climate **15**, 3069-3081.

Reichert, B.K., L. Bengtsson, J. Oerlemans, 2002: Recent Glacier Retreat Exceeds Internal Variability. - Journal of Climate **14**, 3767-3784.

Rogers, J.C., H. Van Loon, 1979: The Seesaw in Winter Temperatures between Greenland and Northern Europe. Part II: Some Oceanic and Atmospheric Effects in Middle and High Latitudes. - Monthly Weather Review **107**, 509–519.

Schneeberger, C., O. Albrecht, H. Blatter, M. Wild, R. Hock, 2001: Modelling the response of glaciers to a doubling in atmospheric CO_2: a case study of Storglaciären, northern Sweden. - Climate Dynamics **17**, 825-834.

Schönwiese, C., 2006: Praktische Statistik für Meteorologen und Geowissenschaftler – Borntraeger, Berlin, Stuttgart, 302.

Schuler, T.V., R. Hock, M. Jackson, H. Elvehøy, M. Braun, I. Brown, J.-O. Hagen, 2005: Distributed mass-balance and climate sensitivity modelling of Engabreen, Norway – Annals of Glaciology **42**, 395-401.

Sivia, D.S., J. Skilling, 2006: Data Analysis - A Bayesian Tutorial. - Oxford University Press, New York.

Six, D., L. Reynaud, A. Letréguilly, 2001: Bilans de masse des glaciers alpins et scandinaves, leurs relations avec l'oscillation du climat de l'atlantique nord. - Sciences de la Terre et des planètes / Earth and Planetary Sciences **333**, 693-698.

SSB 2012: Electricity, annual figures, 2011: http://www.ssb.no/en/elektrisitetaar/, last accessed on 10.04.2013.

Tebaldi, C., R.L. Smith, D. Nychka, L.O. Mearns, 2005: Quantifying Uncertainty in Projections of Regional Climate Change: A Bayesian Approach to the Analysis of Multimodel Ensembles. - Journal of Climate **18**, 1524–1540.

Teisserenc De Bort, L.P., 1883: Etude sur l'hiver de 1879-80 et recherches sur l'influence de la position des grands centres d'action de l'atmosphère dans les hivers anormaux. - Ann. de la Soc. Météor. de France **31**, 70-79.

Uppala, S. M., P. W. Kallberg, A. J. Simmons, U. Andrae, V. D. C. Bechtold, M. Fiorino, J. K. Gibson, J. Haseler, A. Hernandez, G. A. Kelly, X. Li, K. Onogi, S. Saarinen, N. Sokka, R. P. Allan, E. Andersson, K. Arpe, M. A. Balmaseda, A. C. M. Beljaars, L. Van de Berg, J. Bidlot, N. Bormann, S.

Caires, F. Chevallier, A. Dethof, M. Dragosavac, M. Fisher, M. Fuentes, S. Hagemann, E. Hólm, B. J. Hoskins, L. Isaksen, P. A. E. M. Janssen, R. Jenne, A. P. Mcnally, J.-F. Mahfouf, J.-J. Morcrette, N. A. Rayner, R. W. Saunders, P. Simon, A. Sterl, K. E. Trenberth, A. Untch, D. Vasiljevic, P. Viterbo & J. Woollen, 2005: The ERA-40 re-analysis. - Quarterly Journal of the Royal Meteorological Society **131**(612), 2961–3012.

Van Loon, H., J.C. Rogers, 1978: The Seesaw in Winter Temperatures between Greenland and Northern Europe. Part I: General Description. - Monthly Weather Review **106**, 296–310.

Von Storch, H., F. Zwiers, 1999: Statistical analysis in climate research. – Cambridge University Press, Cambridge, 496.

Walker, G.T., 1924: 'Correlations in seasonal variations of weather IX'. - Memoirs of the India Meteorological Deptartment **24**, 275–332.

Walker, G.T., E.W. Bliss, 1932: World Weather V. - Memoirs of the Royal Meteorological Society **4**(36), 53–84.

Washington, R., A. Hodson, E. Isaksson, O. Macdonald, 2000: Northern hemisphere teleconnection indices and the mass balance of Svalbard glaciers. - International Journal of Climatology **20**, 473-487.

Watson, E., B.H. Luckman, B.Yu, 2006: Long-term relationship between reconstructed seasonal mass balance at Peyto Glacier, Canada, and Pacific sea surface temperatures. - The Holocene **16**, 873-790.

Weber, M., L. Braun, 2004: Ursachen des Gletscherschwunds in den Alpen. - Geographische Schule **26**(148), 21-27.

Wilks, D., 2006: Statistical methods in the atmospheric sciences – Elsevier Academic Press, Amsterdam, 648.

Winkler, S., 1996: Front variations of outlet glaciers from Jostedalsbreen, western Norway, during the twentieth century. - Norges Geologiske Undersøkelse Bulletin **431**, 33-47.

Winkler, S., 1997: Der aktuelle Gletschervorstoß in Westnorwegen – Ursachen und Ablauf – Gletscherwachstum trotz “global warming”? - NORDEN **12**, 181-203.

Winkler, 2009: Gletscher und ihre Landschaften – eine illustrierte Einführung. - Pumusverlag, Darmstadt.

Winkler, S., T. Chinn, I. Gärtner-Roer, S.U. Nussbaumer, M. Zemp, H.J. Zumbühl, 2010: An introduction to mountain glaciers as climate indicators with spatial and temporal diversity. - Erdkunde **64**, 97-118.

Winkler, S., H. Elvehøy, A. Nesje, 2009: Glacier fluctuations of Jostedalsbreen, western Norway, during the past 20 years: the sensitive response of maritime mountain glaciers. - The Holocene **19**, 395–414.

Winkler, S., N. Haakensen, A. Nesje, N. Rye, 1997: Glaziale Dynamik in Westnorwegen – Ablauf uns Ursachen des aktuellen Gletschervorstoßes am Jostedalsbreen. - Petermanns Geographische Mitteilungen **141**, 43-63.

Winkler, S., N. Haakensen, 1999: Kritische Überprüfung der Möglichkeit zur Prognose des Gletscherverhaltens auf Grundlage von Modellierungen – dargestellt anhand von regionalen Beispielen aus Norwegen. - Petermanns Geographische Mitteilungen **143**, 291-304.

Winkler, S., A. Nesje, 2009: Perturbation of Climatic Response at Maritime Glaciers. - Erdkunde **63**, 229-244.

Zemp, M., W. Haeberli, M. Hoelzle, F. Paul, 2006: Alpine Glaciers to disappear within decades? - Geophysical Research Letters **33**, L13504.

Acknowledgements

The present study was carried out at the Institute of Geography and Geology of the University of Würzburg within the DFG funded project DYNAMO-KG. Therefore, I would like to acknowledge the German Research Foundation (Deutsche Forschungsgemeinschaft, DFG) for the financial support. I also acknowledge the modelling groups, the Program for Climate Model Diagnosis and Intercomparison (PCMDI) and the WCRP's Working Group on Coupled Modelling (WGCM) for their roles in making available the WCRP CMIP3 multi-model dataset, and the Office of Science, U.S. Department of Energy, who provide support for this dataset. Furthermore, I acknowledge the Norwegian Water Resources and Energy Directorate (Norges vassdrags- og energidirektorat, NVE) for providing the glacier mass balance data used in this study, the European Centre for Medium-Range Weather Forecasts (ECMWF) for providing the ERA40 re-analysis data and National Centers for Environmental Prediction (NCEP) and the National Center for Atmospheric Research (NCAR) for making their re-analysis products available.

Personally, I would like to thank my supervisors Prof. Dr. Heiko Paeth and PD Dr. Stefan Winkler for their professional advice, competent guidance and continued friendly support throughout the duration of this project and beyond. In addition, I would like to express my gratitude to my friends and former colleagues Andreas Paxian and Gernot Vogt, with whom I spent many hours discussing our work and exchanging ideas. I am also very thankful for the friendly work atmosphere granted by the whole working group at the Institute of Geography and Geology. Finally, I deeply thank my family and my partner Melanie Rieß for their encouragement and emotional support.

Erklärung

Hiermit versichere ich, Sebastian Mutz, geboren am 17.04.1987 in Selb, dass ich die vorliegende Arbeit selbstständig verfasst und keine anderen als die angegebenen Quellen und Hilfsmittel benutzt habe, dass alle Stellen der Arbeit, die wörtlich oder sinngemäß aus anderen Quellen übernommen wurden, als solche kenntlich gemacht sind und dass die Arbeit in gleicher oder ähnlicher Form noch keiner Prüfungsbehörde vorgelegt wurde.

Würzburg, Mai 2013